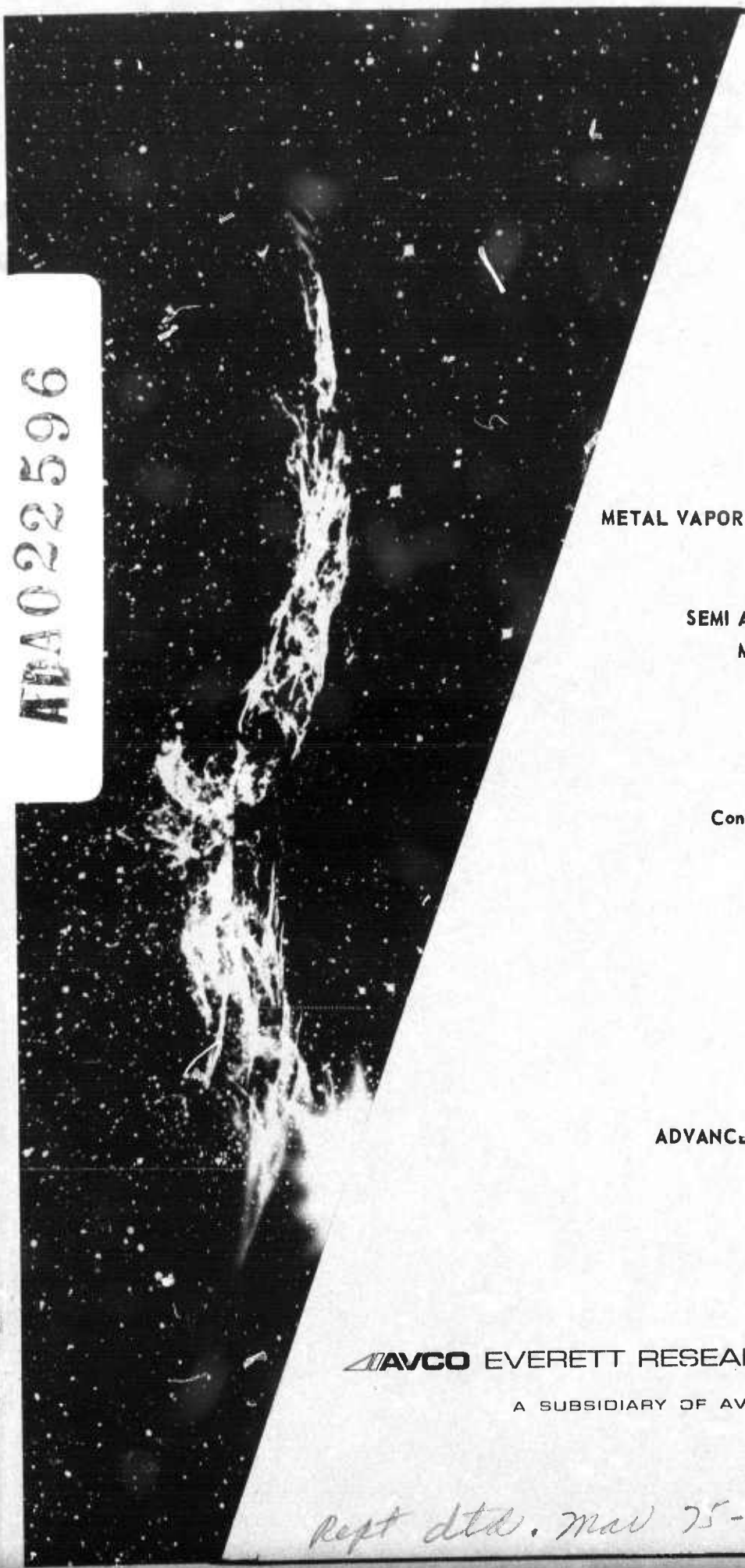

12 DRT

METAL VAPOR VISIBLE LASER KINETICS PROGRAM

SEMI ANNUAL TECHNICAL REPORT

March 1975 – August 1975

Contract No. N00014-75-C-0061

February 1976

sponsored by

ADVANCED RESEARCH PROJECTS AGENCY

ARPA Order No. 1806

AVCO EVERETT RESEARCH LABORATORY, INC.

A SUBSIDIARY OF AVCO CORPORATION

Rept dtd. Mar 75 - AD A014679

UNCLASSIFIED

SECURITY CLASSIFICATION OF THIS PAGE (When Data Entered)

REPORT DOCUMENTATION PAGE

READ INSTRUCTIONS BEFORE COMPLETING FORM

1. REPORT NUMBER

2. GOVT ACCESSION NO.

3. RECIPIENT'S CATALOG NUMBER

4. TITLE (and Subtitle)

METAL VAPOR VISIBLE LASER KINETICS PROGRAM,

5. TYPE OF REPORT & PERIOD COVERED

Semi-Annual Technical Rpt. March 1975 - August 1975

6. PERFORMING ORG. REPORT NUMBER

7. AUTHOR(s)

D. Trainor, A. Mandl and H. Hyman

8. CONTRACT OR GRANT NUMBER(s)

N00014-75-C-0061
ARPA Order-1806

9. PERFORMING ORGANIZATION NAME AND ADDRESS

Avco Everett Research Laboratory, Inc.
2385 Revere Beach Parkway
Everett, Massachusetts 02149

10. PROGRAM ELEMENT, PROJECT, TASK AREA & WORK UNIT NUMBERS

11. CONTROLLING OFFICE NAME AND ADDRESS

Advanced Research Projects Agency
ARPA Order No. 1806

12. REPORT DATE

February 1976

13. NUMBER OF PAGES

97

14. MONITORING AGENCY NAME & ADDRESS (if different from Controlling Office)

Office of Naval Research
Department of the Navy
Arlington, Virginia 22217

15. SECURITY CLASS. (of this report)

Unclassified

15a. DECLASSIFICATION/DOWNGRADING SCHEDULE

16. DISTRIBUTION STATEMENT (of this Report)

97p.

17. DISTRIBUTION STATEMENT (of the abstract entered in Block 20, if different from Report)

18. SUPPLEMENTARY NOTES

19. KEY WORDS (Continue on reverse side if necessary and identify by block number)

1. Electronic State Collisional Relaxation Kinetics
2. Metastable Atom Quenching
3. Temperature Dependence of Metastable Atom Relaxation
4. Electronically Excited Lead Atoms
5. Electronically Excited Copper Atoms
6. Resonance Fluorescence
7. Resonance Absorption
8. Electron Excitation Cross Sections
9. Electron Mixing Cross Sections
10. Electronically Excited Bismuth Atoms

20. ABSTRACT (Continue on reverse side if necessary and identify by block number)

Objective: The objective of this program is to investigate experimentally and theoretically the important kinetic rate processes pertinent to the development of a high power visible laser. This research consists of three tasks. Each of the tasks are summarized below.

TASK I - LOWER LEVEL KINETICS (EXPERIMENTAL)

Objective: The purpose of this task is to identify metal atom systems that allow selective collisional relaxation processes to efficiently quench lower

DD FORM 1 JAN 73 1473 EDITION OF 1 NOV 65 IS OBSOLETE

UNCLASSIFIED 048450

SECURITY CLASSIFICATION OF THIS PAGE

(20)
levels of potential or actual laser transitions. The present experimental study is directed to kinetic rate constant measurements for collisional relaxation of low-lying optically metastable states of lead, copper and bismuth.

Accomplishments: The high temperature flash photolysis apparatus developed under this contract was used to provide collisional quenching rate constants for deactivation of the $^2D_{5/2}$ state of copper (the lower laser level of the 5106 Å green laser transition) at 600°K. The apparatus is now being modified to provide temperature-dependent rate constant data for collisional deactivation of two low-lying optically metastable states of bismuth.

TASK II - UPPER LEVEL KINETICS (EXPERIMENTAL)

Objective: The purpose of this task is to determine the efficiency of various quenching gases in deactivating the upper laser level of lead. To be useful, a quenching gas must rapidly relax the lower laser level and slowly relax the upper laser level, i.e., be selective.

Accomplishments: A new experimental high-temperature resonance fluorescence apparatus was constructed under this contract. Utilizing DC phase sensitive detection techniques, cross-section information was provided for quenching of the 6p 7s $^3P_1^o$ state of atomic lead – the upper laser level of the 4058 Å laser transition.

TASK III - EXCITATION PROCESSES (THEORETICAL)

Objective: The objective of this effort is to calculate electron impact excitation and quenching cross section for the upper and lower laser levels of copper.

Accomplishments: Important cross sections required for modeling the copper vapor laser were calculated. These results, when applied to modeling the laser's performance, predict that a larger number of atoms are capable of being utilized for lasing, with a correspondingly higher laser energy density and a greater overall system efficiency.

FOREWORD

ARPA Order Number: 1806

Program Code Number: 5E20

Name of Contractor: Avco Everett Research Laboratory, Inc.

Effective Date of Contract: August 15, 1974

Contract Expiration Date: June 14, 1976

Amount of Contract: $301,042

Contract Number: N00014-75-C-0061

Principal Investigator and Phone Number: Dr. D. Trainor
(617) 389-3000, Ext. 467

Scientific Officer: Director, Physics Program
Physical Sciences Division
Office of Naval Research
Department of the Navy
800 North Quincy Street
Arlington, Virginia 22217

Short Title of Work: Visible Metal Vapor Laser Kinetics

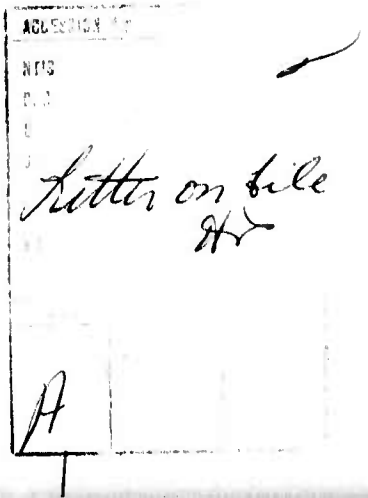

TABLE OF CONTENTS

LIST OF ILLUSTRATIONS

TASK I

LOWER LEVEL KINETICS

1.1 INTRODUCTION

This task provides a kinetic data base to assess the likely suitability of various metal atoms as candidates for the construction of a high power, efficient visible laser. It consists of three subtasks, identified as to the particular metal atom under consideration, namely: (1) a measurement of the temperature dependence from 300 - 600°K of collisional relaxation rate constants for the $6p^2$ ($^3P_2$) and ($^3P_1$) states of atomic lead; (2) similar measurements for the $3d^9\ 4s^2$ ($^2D_{5/2}$) and ($^2D_{3/2}$) states of atomic copper at temperatures near 600°K; and recently under a contract modification (3) temperature dependent information on the $6p^3$ ($^2D^o_{3/2}$) and ($^2D^o_{5/2}$) states of Bismuth.

1.2 TEMPERATURE DEPENDENT LEAD RELAXATION EXPERIMENTS

This subtask was completed and the results reported in the March 1975 Semi-Annual Technical Report. These results were also presented at the 169th National American Chemical Society Meeting in Philadelphia (April 1975) and accepted for publication in the Journal of Chemical Physics. A copy of this technical paper is included as Appendix A of this report. The laser implications of these lower level quenching results combined with the upper level measurements (see Task II, this report), with regard to a number of viable lead laser concepts, will be discussed in the last section of this report, entitled "Laser Implications".

1.3 COLLISIONAL RELAXATION OF ELECTRONICALLY EXCITED COPPER

The purpose of this subtask was to provide quenching rate constant information for the lower laser levels of the 5106 Å (green) and 5782 Å (yellow) transition in copper. These states are the optically metastable $3d^9\ 4s^2$ ($^2D_{5/2}$) and ($^2D_{3/2}$) states, respectively. The experimental approach was to utilize the high temperature flash photolysis cell which successfully provided information on the lead metastable states in an analogous manner on copper. There were a number of important differences, however, between these two systems that made the copper experiments considerably more difficult than the lead, namely: (1) there was no established high vapor pressure organo-metallic copper compound analogous to tetramethyl lead available for use as a photolytic precursor of the copper metastable states; (2) this caused us to utilize the copper (I) halides, i.e., the chloride and iodide salts, as photolytic precursors of these metastable states. Since these salts exist as solids at room temperature, to generate a sufficient vapor pressure of the compound, all surfaces in contact with the gas mixtures had to be maintained at a uniform, elevated temperature near 600°K. Finally, (3) there also was not available a strong transition terminating on the $^2D_{3/2}$ state which could be utilized to probe the production and subsequent decay of the state as produced in our flash apparatus. The end result of these complications was that kinetic rate constant information could be obtained only for the $^2D_{5/2}$ state – the lower laser level for the 5106 Å (green) transition. These kinetic rate constant results have been reported at the 2nd Summer Colloquium on Electronic Transition Lasers held in Woods Hole, Massachusetts (September 1975), and have been submitted as

a technical paper to the Journal of Chemical Physics. A copy of the submitted version is included as Appendix B of this report.

Although no direct observation of any photoproduction of the $^2D_{3/2}$ state of copper was encountered in these flash photolysis experiments, it most likely was produced in the flash discharge and was undetectable in our apparatus due to the poor signal/noise encountered for our light source/detection system and the relatively weak transition probability for the available probe line. There was, however, some indirect evidence that it was indeed produced and this evidence suggested an invention which utilizes electronic-to-vibrational energy transfer processes to selectively allow the copper vapor laser to be more easily operated on the yellow rather than the green transition by using carbon monoxide as a quenching gas. A disclosure of invention was submitted on this idea in October 1975. The basic characteristics of this concept and available experimental evidence to support this model are summarized as follows.

It was established (see Appendix B) that in our heated (550 - 620°K) reaction cell, when flash mixtures containing 50 torr of Ar and 0.5 μ of copper halides were photolyzed (flashlamp energies near 400 joules), some photo-production of the $^2D_{5/2}$ state was observed using resonance absorption techniques. When carbon monoxide, CO, was added to these mixtures, several features in the production and decay of the $^2D_{5/2}$ state were observed: (1) there was an increase in the absorption of the 2824 Å resonant line chosen to monitor the production of the $^2D_{5/2}$ state suggesting an apparent increase in concentration of this state; (2) the CO had little effect on the observed time-resolved decay of the $^2D_{5/2}$ state suggesting it

to be an inefficient deactivator of the $^2D_{5/2}$ state of copper; and (3) there was no evidence (within the experimental scatter of the data) of any deviation in the decay from the expected simple first-order decay characteristics. This observation is consistent with the absence of any slow cascade processes populating this low-lying level by feeding from an upper state. It is this last point which requires further exploration since it is the basis of the suggestion that CO is an efficient quencher of the $^2D_{3/2}$ state, i.e., CO rapidly and efficiently deactivates the $^2D_{3/2}$ state through a likely E→V process with the copper terminating principally in the $^2D_{5/2}$ state and the CO excited by one vibrational quantum.

The nature of the experimental apparatus is that for times of approximately 150 μsec from initiation of the experiment (discharge of the capacitors to fire the flashlamps), no signal is monitored by the atomic resonance detection system because of a mechanical shutter which blocks the light source from being observed by a combined monochromator/photomultiplier/oscilloscope arrangement. This shutter is utilized to prevent the intense flashlamp light output from saturating the photomultiplier and thereby rendering it unreliable to make atomic resonance absorption measurements. Therefore, any fast cascading process should likely have undergone perhaps three characteristic decay times in the time period during which no observations were made, i.e., during the 150 μsec that the light source is blocked, all cascading processes would have essentially gone to completion, for example,

$$^3\tau_{CHAR} = \frac{3}{k_L [CO]} = 150 \times 10^{-6} \text{ sec}$$

for [CO] equal to 6.6×10^{16} particles/cm^3, then $k_L = 3 \times 10^{-13}$ cm^3/sec. The (calculated) magnitude of this rate constant is modest for processes involving E→V energy transfer but is of correct magnitude to be useful as a deactivator of the lower laser level between excitation pulses. In general, the quenching gas chosen to deactivate these metastable states should have the following properties: (1) it should be an efficient quencher and thereby be utilized in small mole fractions of the total laser mixture. This would tend to minimize its effect on the electrical characteristics of the laser discharge; (2) it should be selective, such that its rate of deactivation of the upper laser level doesn't compete with stimulated emission, or the laser's efficiency would be reduced.

As an approximation, for a quenching gas to have little effect on the upper laser level, the rate of deactivation should be less than the inverse of the time of the pulse duration, which for electric copper lasers implies

$$k_u[Q] < (20 \times 10^{-9} \text{ sec})^{-1}$$

where k_u is a rate constant describing deactivation of the upper laser level through collision with quenchers, Q. To place a limit on the density of Q useful for laser operation, one may set k_u equal to a gas kinetic rate constant (deactivation on every collision), i.e., $k_u \simeq 2 \times 10^{-10}$ cm^3/mole-sec. This suggests

$$[Q] < 2.5 \times 10^{17} \text{ particles/cm}^3.$$

As an approximation take $[Q] = 5 \times 10^{16}$ particles/cm^3. This allows calculation of the magnitude of the rate constant that would be needed to collisionally remove the lower laser metastable state population between subsequent excitation pulses. This density of quenching gas must complete

the deactivation sufficiently so that in the next excitation pulse the production of an inversion is possible. This requires the relaxation time to be compared with the desired pulse repetition frequency, e.g., 20 kHz. Therefore,

$$k_L[Q] \approx 2 \times 10^4 \text{ sec}^{-1}$$

where k_L is a rate constant describing deactivation of the lower laser level through collisions with quenchers, Q. For our example where $[Q] = 5 \times 10^{16}$ particles/cm^3, then $k_L \approx 4 \times 10^{-13}$ cm^3/sec. Leone and Wodarczyk (see Appendix A; Ref. A-10) studied the process

$$Br(^2P_{1/2}) + HX(v=o) \rightarrow Br(^2P_{3/2}) + HX(v=1) + \Delta E$$

and found k equal to approximately 7 and 50 x 10^{-13} cm^3/sec for collisional relaxation by HBr and HCℓ, respectively. These E→V processes are exothermic by 1125 and 800 cm^{-1}, respectively for HBr and HCℓ. We have found similar fast rate constants in our experiments on lead for those cases where likely E→V processes were occurring. This information is relevant to the invention described here since it is proposed that carbon monoxide processes these desired characteristics with regard to the yellow copper laser transition. It is further suggested that this efficient quenching occurs via an endothermic near-resonant electronic-to-vibrational energy transfer process, viz.

$$Cu\ ^2D_{3/2} + CO(v=o) + \Delta E = 101 \text{ cm}^{-1} \rightarrow Cu\ ^2D_{5/2} + CO(v=1).$$

In summary, CO is likely to be an efficient, selective deactivator of the $^2D_{3/2}$ state of copper proceeding to remove these metastable states through likely E→V energy transfer processes at rates sufficiently fast to

effectively allow high pulse repetition frequencies. At the same time it would likely stifle lasing in the green, due to increased $^2D_{5/2}$ state production through cascading and inefficient collisional deactivation of the $^2D_{5/2}$ states. These predictions were qualitatively supported by preliminary experiments conducted at AERL on an electric discharge copper laser constructed under an IRAD program.

1.4 TEMPERATURE DEPENDENT BISMUTH RELAXATION EXPERIMENTS

The results of this subtask will be discussed in future reports as no progress has been accomplished during this report period.

TASK II

UPPER LEVEL KINETICS

This task addresses the question of whether the quenching gases that efficiently deactivated the lower metastable states of lead were inefficient in deactivating the upper laser level, i.e., the 6p 7s $^3P_1^o$ state of lead. To be useful, a quenching gas must be selective. This experimental task was successfully completed during this contract period and the results will be published in Physical Review A. A copy of the submitted version of this paper is attached as Appendix C.

TASK III

ELECTRON IMPACT CROSS SECTIONS RELEVANT TO THE COPPER VAPOR LASER

3.1 INTRODUCTION

A knowledge of electron impact excitation and quenching cross sections is of fundamental importance for modeling the copper vapor laser.[1] The only data in the literature on the required cross sections for copper is the recent work of Williams and Trajmar.[2] These authors have measured cross sections for direct excitation from the ground state to the upper and lower laser levels at electron impact energies of 20 eV and 60 eV. However, no data exists at lower energies, and no measurements whatsoever have been made for the cross section for collisional mixing (quenching) of the two laser levels due to electron impact. As far as we are aware, the only other relevant, published information is the early theoretical work of Leonard,[3] who made estimates of the direct excitation and mixing rates using purely classical, Gryzinski-type methods. Although such methods may be useful for strongly-allowed transitions, they are of dubious validity for treating the excitation of the metastable lower laser level or for the very weakly-allowed mixing transition. Leonard's direct excitation cross sections are found to be about an order-of-magnitude smaller than the absolute values given by Williams and Trajmar. In view of this large discrepancy, and of the lack of relevant data in general, we have undertaken a theoretical investigation of the required cross sections.

Figure 1 shows a partial energy level diagram for the copper atom, indicating the laser transitions. The lower, ^2D levels are metastable, with lifetimes ~20 sec. The laser operates on the very weakly-allowed transition $3d^{10}4p \rightarrow 3d^9 4s^2$ ($f \sim 5 \times 10^{-3}$), which is a "2-electron jump" and therefore takes place due to configuration interaction effects. In the next section, we consider the calculation of the cross sections for the following three transitions (see Fig. 1): 1) direct excitation of the upper laser level, $3d^{10}4s\ ^2S \rightarrow 3d^{10}4p\ ^2P$, 2) direct excitation of the lower level, $3d^{10}4s\ ^2S \rightarrow 3d^9 4s^2\ ^2D$ (we have not resolved the J = 5/2, 3/2 sublevels in the calculation, but these individual cross sections should be approximately in the ratio of their respective statistical weights), and 3) the collisional mixing process $3d^9 4s^2\ ^2D \rightarrow 3d^{10}4p\ ^2P$ (which, by detailed balance, can be simply related to the quenching process $^2P \rightarrow {}^2D$).

3.2 CALCULATIONS

A. Upper Laser Level

The calculations for the transition $3d^{10}4s\ ^2S \rightarrow 3d^{10}4p\ ^2P$ were based upon the symmetrized and unitarized, impact parameter theory.[4, 5] Although this method is very simple to apply, it has proven to be quite reliable for optically-allowed, atomic transitions. The success of the method is due to the long-range nature of the dipole interaction, which allows the transition amplitude to build up while the colliding electron is relatively far from the target atom. The cross section is thus not very sensitive to the details of the atomic field at small radial distances, where an accurate theoretical treatment becomes more difficult.

The theory is worked out in detail in Refs. 4 and 5, and only a brief discussion is included here. The basic, working formula is

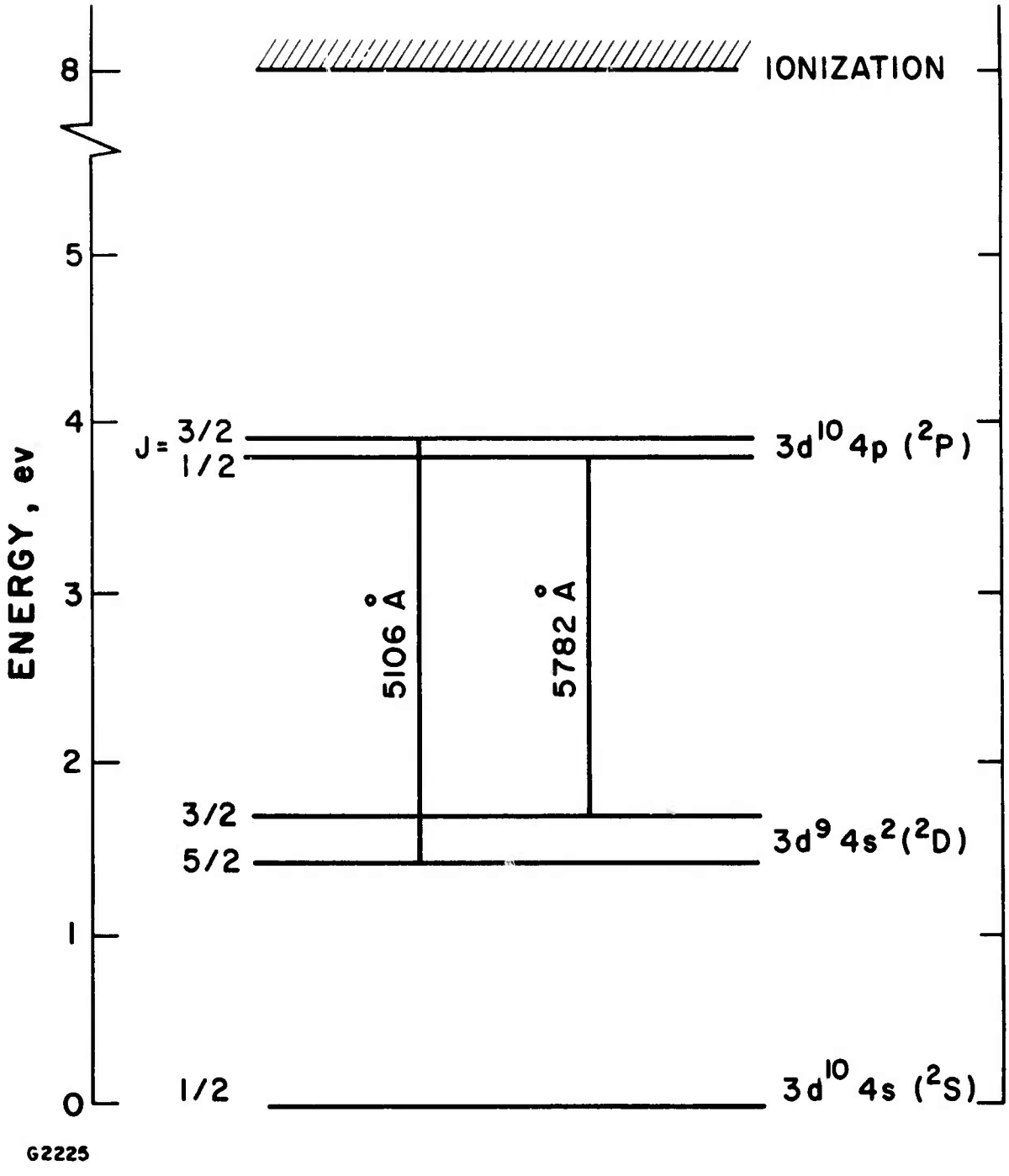

Fig. 1 Partial Energy Level Diagram for Copper

$$Q_{ij} = \int_{R_o}^{\infty} P_{ji}(R_i)\, 2\pi R_i dR_i = 1480\, \frac{f_{ji}}{E_i \Delta E}\, \phi(\beta_o)\, \pi a_o^2 \qquad (1)$$

with $\beta_o = .271 \sqrt{E_i}\ R_o\, \Delta E/(E_i + E_j)$, and where Q_{ij} is the cross section for excitation from state i to j, $P_{ji}(R_i)$ is the probability for the transition to take place at a given impact parameter R_i, f_{ji} is the optical oscillator strength, R_o is the impact parameter cut-off radius, ΔE is the transition energy, and E_i, E_j are the initial and final energies of the colliding electron, respectively (all energies are in eV). Finally, $\phi(\beta) = \beta K_o(\beta) K_1(\beta)$, where K_n are modified Bessel functions; the function ϕ is tabulated for convenience in Ref. 4. The formula for Q_{ij} must be modified somewhat[4] in order to conserve flux if $P \geq 1/2$ for some $R_i > R_o$. The only unknown is therefore the parameter R_o. If $\bar{r}_i$, $\bar{r}_j$ denote the mean radii of the optical electron in states i and j, respectively, then Seaton[4] has suggested using $R_o = \bar{r}_<$, where $\bar{r}_<$ is the smaller of $\bar{r}_i$, $\bar{r}_j$, while Stauffer and McDowell[5] have used a suitably-weighted average value. We have found, however, that for excitation of the resonance transition in metal atoms, the best results in the low to intermediate energy range are obtained with the choice $R_o = \bar{r}_>$, with $\bar{r}_>$ the larger of $\bar{r}_i$, $\bar{r}_j$; it should be noted that this is in fact the most stringent condition on the theory. The required values of $\bar{r}_>$ were estimated from the quantum defect formula,[6] $\bar{r}_> = [3n^{*2} - \ell(\ell+1)]/2$, which should be adequate for the excited states.

As examples, the method has been applied to excitation of the $3p^2P$ level in Na and of the $4s4p\,^1P$ level in Ca, since accurate absolute experimental cross sections exist for both of these cases. For Na we used $R_o = \bar{r}_> = 5.72\, a_o$, while for Ca we took $R_o = \bar{r}_> = 5.41\, a_o$. The

theoretical results are given as the solid curves in Fig. 2; the dashed curves are the experimental cross sections measured by Gallagher and co-workers.[7,8] It should be pointed out that the agreement for the Ca case is somewhat misleading, since the experimental curve includes cascade contributions, and is therefore estimated[8] to be about 15-30% too high in the energy range of interest. Nevertheless, reasonable agreement (within a factor of 2) is obtained between theory and experiment.

Formula (1) has been applied to the excitation of the upper laser level in copper, with the parameter R_o taken to be 4.21 a_o. The result of the calculation is the solid curve, labeled ^2P, in Fig. 3, while the open circles are the absolute values given by Williams and Trajmar. The actual measurements of these authors yield relative cross sections, since it is extremely difficult to make an absolute measurement for Cu in their apparatus. To normalize their data, they extrapolated to zero momentum transfer, where the generalized oscillator strength can be equated to the known optical f-value. In addition, the integral elastic cross section was compared to an approximate, theoretical value;[9] both methods gave reasonable agreement. Nevertheless, at 20 eV and 60 eV, the present theory is expected to be quite accurate, certainly to well within a factor of 2. Thus, although our results have no bearing on the relative cross sections measured by Williams and Trajmar, they do suggest a renormalization of the absolute scale. Very recently, Cartwright and co-workers[10] have recalculated the integral elastic scattering cross section for Cu at 60 eV, using a more sophisticated distorted waves theory. Their results indicate that the normalization factor used by Williams and Trajmar at 60 eV is over an order-of-magnitude too high, thus lending support to the present findings.

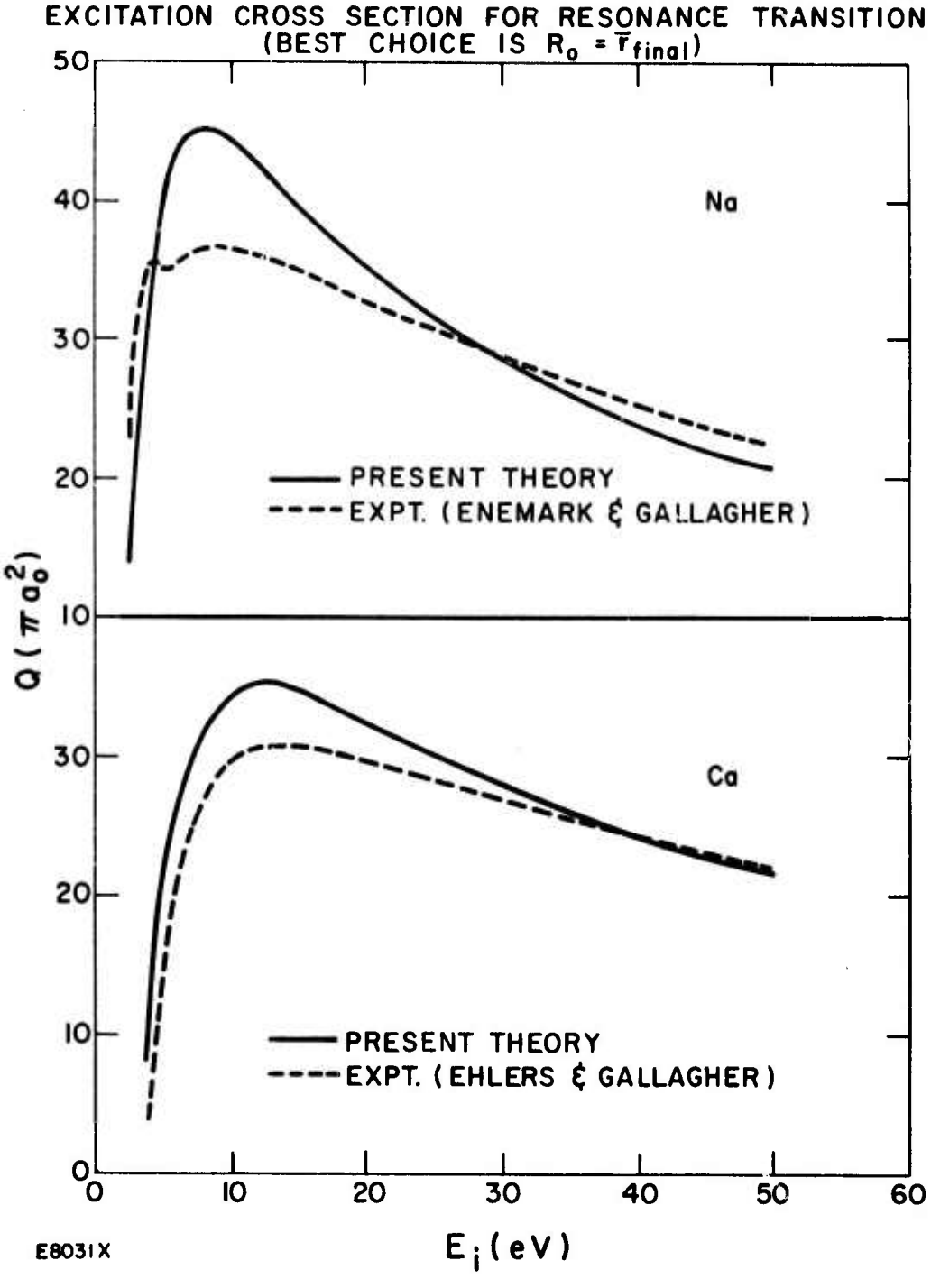

Fig. 2 Electron Impact Excitation Cross Sections for the Resonance Levels of Sodium and Calcium. Solid curves: present theory; dashed curves: experiment.[7, 8]

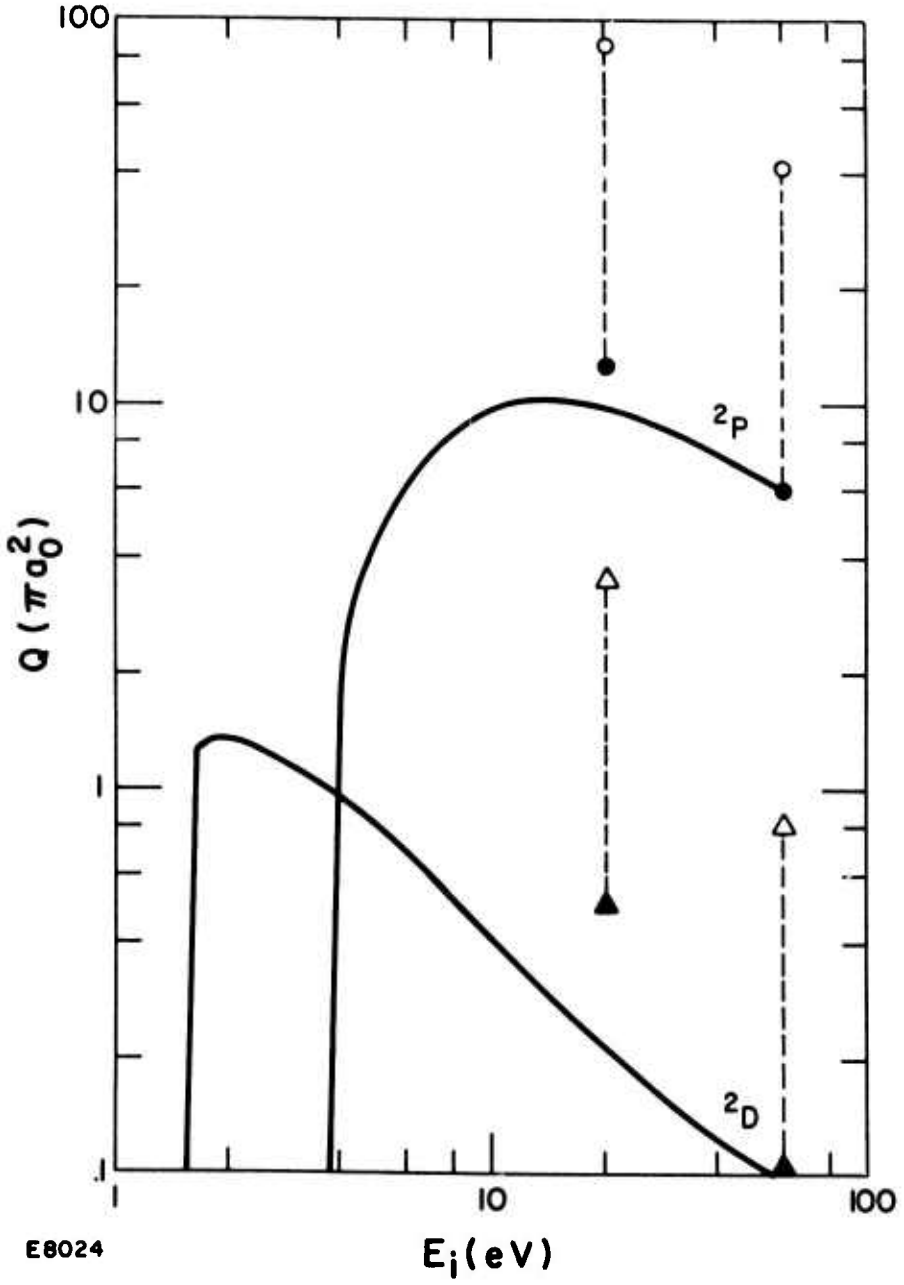

Fig. 3 Direct Electron Impact Excitation of the Upper (^2P) and Lower (^2D) Copper Laser Levels. Solid curves: present theory; open circles: ^2P absolute cross section from Ref. 2 [closed circles: renormalized data (see text)]; open triangles; ^2D absolute cross section from Ref. 2 [closed triangles: renormalized data (see text)].

Our values are also in reasonable agreement with Leonard's original estimates.[3] At 60 eV, where the theory is expected to be the most reliable, the ratio of the experimental[2] to calculated value is a factor of 7, and we have thus renormalized the data by this factor. The procedure shifts the open circles downward to the closed circles, as shown in Fig. 3. The agreement between the renormalized value and the theoretical result at 20 eV is seen to be very good (within 25%). Finally, it should be noted that sharp resonance features may appear in the cross section at energies below the ionization threshold. Predicting this type of complicated structure is clearly beyond the scope of the present investigation.

B. Lower Laser Level

The lower laser level is metastable, and thus the transition $3d^{10}4s\ ^2S \rightarrow 3d^9 4s^2\ ^2D$ is optically forbidden. In general, forbidden transitions are difficult to treat due to the short-range nature of the interaction involved. However, Stauffer and McDowel[5,11] have generalized Seaton's original impact parameter theory[4] to the special case of a quadrupole transition, which is spin-allowed and for which $\Delta \ell = 2$. This, fortunately, is exactly the case of interest to us. The appropriate cross-section formula, analogous to expression (1) for the dipole case, can be written in the form

$$Q_{ij} = \frac{1}{5}\left(\frac{\Delta E^2}{\overline{E}_i\, \overline{E}}\right) \frac{S_q^{LS}}{(2L_i + 1)(2S + 1)} \quad \psi(\beta_o)\ \pi a_o^2 \qquad (2)$$

with ΔE, E_i, and β_o defined as before, and where $\overline{E} = (E_i + E_j)/2$, S_q^{LS} is the quadrupole multiplet strength[12] in LS-coupling, and $(2L_i + 1)(2S + 1)$ is the initial-state degeneracy. The function ψ is tabulated in Ref. 11, and is given by $\psi(\beta) = \phi(\beta) + K_1^2(\beta)/2$. The multiplet strength can be written more explicitly as[12]

$$S_q(SL, SL') = \frac{2}{3}(2S + 1) |\langle SL| |T^{(2)}| |SL'\rangle|^2$$

where the last factor is the reduced matrix element expressed in terms of the appropriate tensor operator. To evaluate the reduced matrix element we have used Eq. (9) of Ref. 13; this however requires a knowledge of the radial integral

$$s_q^2 = \left[\int_o^\infty dr\, r^2 P_{3d}(r) P_{4s}(r)\right]^2$$

A good estimate for this integral can be obtained from Garstang's calculations on forbidden transition lifetimes.[14] For the transition $3d^{10} \rightarrow 3d^9 4s$ in nickel (Z = 28), he has determined the value of s_q to be -2.9. Copper (Z = 29) has one more 4s electron, which will provide some additional screening, thereby making s_q somewhat larger; we have therefore adopted the value $s_q^2 = 10$. In addition, we again need to know R_o, the impact parameter cutoff. Since this transition essentially involves an inner-shell rearrangement, we have taken R_o to be the ground-state atomic radius, for which we have used the Hartree-Fock mean orbital radius[15] $\bar{r}_{4s} = 2.97\, a_o$. The cross section can now be calculated from formula (2), and the result is given as the solid curve, labeled ^2D, in Fig. 3. The open triangles are the absolute values of Williams and Trajmar, for excitation of the lower level, while the closed triangles are the renormalized quantities. It should be noted that we have applied the same factor of 7, as determined in Section A, for the renormalization. The agreement between the renormalized and calculated quantities at 60 eV is seen to be almost perfect. Although this is no doubt somewhat fortuitous, given the various approximations made in the calculation (see above), it does lend further

support to our contention that the absolute values of Williams and Trajmar are considerably too high. The agreement at 20 eV is within a factor of ~2. For direct excitation of the lower laser level, the present results differ significantly from Leonard's classical cross section[3] in both shape and magnitude.

C. Collisional Mixing

Although the mixing transition $3d^9 4s^2\ ^2D \rightarrow 3d^{10} 4p\ ^2P$ is optically-allowed, it involves a simultaneous change in state of two electrons. Such a transition is again extremely difficult to handle theoretically, since it is very sensitive to complicated configuration interaction (i.e., dynamical correlation) effects. Nevertheless, formula (1) should still be applicable in order to obtain an estimate of the mixing rate. The primary difficulty is the specification of the parameter R_o. Although no data exists at any energy for the copper mixing cross section, recent measurements have been made for an analogous, 2-electron transition ($4s^2\ ^1S \rightarrow 3d4p\ ^1P$) in calcium.[16] The relevant parameters are[17] $f = .07$ and a Hartree-Fock atomic radius[15] of $\overline{r}_{4s} = R_o = 4.22\ a_o$. The resulting theoretical cross section is $Q = .28\ \pi a_o^2$, compared to the experimental value of $Q = .25\ \pi a_o^2$, at $E_i = 12$ eV (the position of the peak). This good agreement provides some justification for using formula (1) for such 2-electron transitions, with R_o taken to be the Hartree-Fock atomic radius. The oscillator strength for the case of Cu was deduced from the work of Cunningham and Link[18], and was determined to be $f = 5.4 \times 10^{-3}$. The fact that this f-value is much smaller than for the calcium case means that the impact parameter theory will be less reliable for the Cu transition, but it should still provide a useful estimate for the cross section. The copper mean

radius was taken to be 3.0 a_o (see Section B), and the calculation was repeated with $R_o = 3.0 \pm 25\%$ in order to obtain a feeling for the corresponding variation in cross section. The results are shown in Fig. 4 where $R_o^{(1)} = 2.25\ a_o$, $R_o^{(2)} = 3.0\ a_o$ and $R_o^{(3)} = 3.75\ a_o$. The total variation produced by the change in R_o is a factor of ~3, which is comparable to the overall expected accuracy of the calculation. If we take $Q \sim .5\ \pi\ a_o^2$, by detailed balance, we obtain a quenching rate $\sim 2 \times 10^{-8}$ cm^3/sec at an electron temperature of 2 eV. By comparison, Leonard's quenching rate,[3] from the classical theory, is $\sim 2 \times 10^{-7}$ cm^3/sec (only the rate, and not the cross section, is given in Ref. 3). Modeling the copper vapor laser with the present rate, rather than with the earlier estimate,[3] would therefore predict that a larger number of atoms are capable of being utilized for lasing, with a correspondingly higher laser energy density, and a greater overall system efficiency.

To summarize, we have calculated the various cross sections required for modeling the copper vapor discharge laser. The calculations are based upon the dipole and quadrupole versions of the impact parameter theory, as developed by Seaton[4] and extended by Stauffer and McDowell.[5, 11] Our results differ in many respects from the existing, although limited, literature, and further work on this system would clearly be desirable.

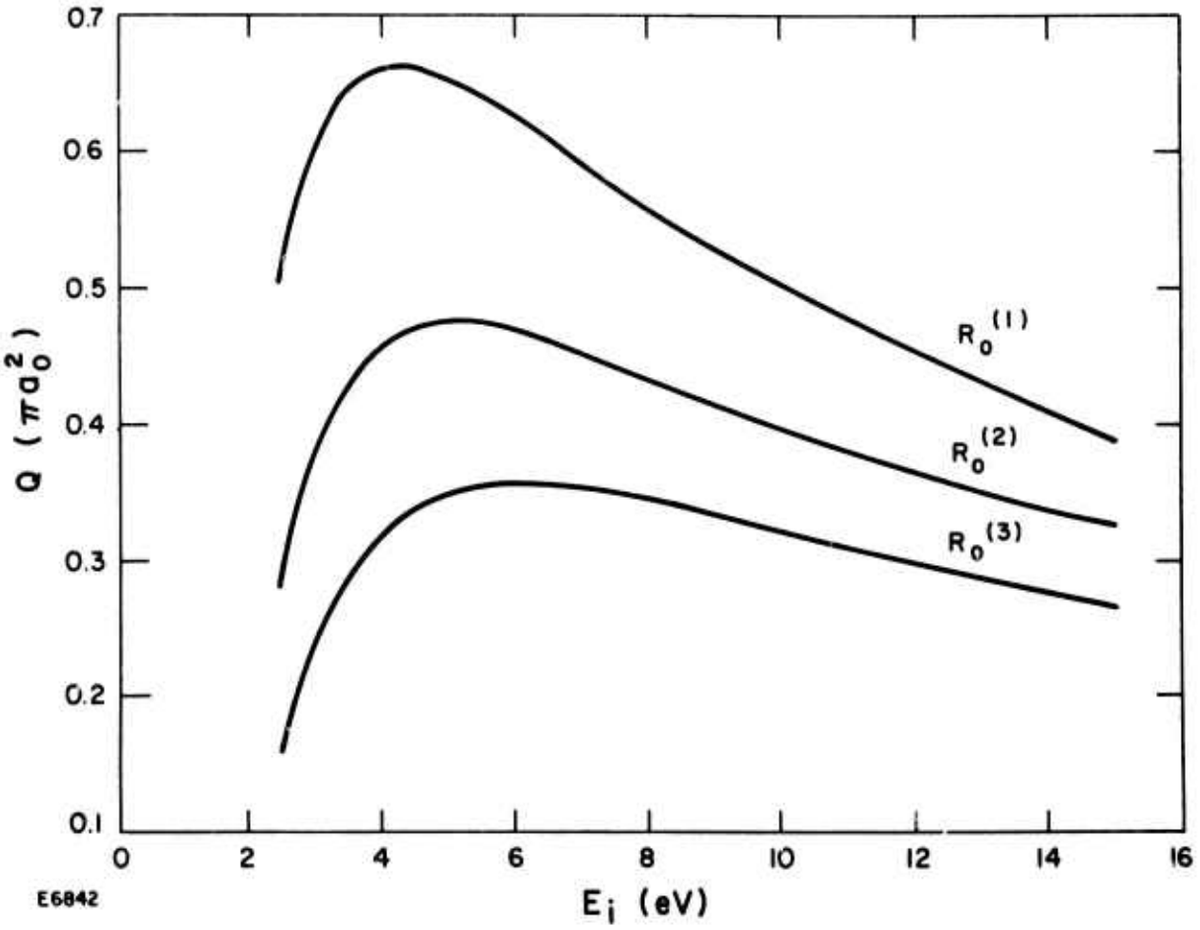

Fig. 4 Collisional Mixing Cross Section for Different Values of the Impact Parameter Cutoff Radius; $R_o^{(1)} = 2.25\ a_o$, $R_o^{(2)} = 3.0\ a_o$, and $R_o^{(3)} = 3.75\ a_o$

REFERENCES

1. G.G. Petrash, Soviet Physics Uspekhi 14, 747 (1972).
2. W. Williams and S. Trajmar, Phys. Rev. Letters 33, 187 (1974).
3. D.A. Leonard, IEEE J. Quant. Elect. 3, 380 (1967).
4. M.J. Seaton, Proc. Phys. Soc. 79, 1105 (1962).
5. A.D. Stauffer and M.R.C. McDowell, Proc. Phys. Soc 89, 289 (1966).
6. E.U. Condon and G.H. Shortley, The Theory of Atomic Spectra, Cambridge University Press, London (1964), p. 117.
7. E.A. Enemark and A. Gallagher, Phys. Rev. A6, 192 (1972).
8. V.J. Ehlers and A. Gallagher, Phys. Rev. A7, 1573 (1973).
9. N. Winter and D.C. Cartwright (unpublished, as reported in Ref. 2).
10. D.C. Cartwright (private communication).
11. A.D. Stauffer and M.R.C. McDowell, Proc. Phys. Soc. 85, 61 (1965).
12. R.H. Garstang, Camb. Phil. Soc. Proc. 53, 214 (1957).
13. R.H. Garstang, Camb. Phil. Soc. Proc. 54, 383 (1958).
14. R.H. Garstang, J. Res. NBS 68A, 61 (1964).
15. C. Froese Fischer, Atomic Data 4, 301 (1972).
16. I.I. Garga, I.S. Aleksakhin, V.P. Starodub, and I.P. Zapesochnii, Opt. Spect. 37, 482 (1974).
17. W.L. Wiese, M.W. Smith, and B.M. Miles, Atomic Transition Probabilities, National Bureau of Standards Pub. No. NSRDS-NBS 22, Vol. II, U.S. GPO, Washington, D.C. (1969).
18. P.T. Cunningham and J.K. Link, J. Opt. Soc. Amer. 57, 1000 (1967).

LASER IMPLICATIONS

LEAD LASER CONCEPTS

One of the metal systems that has been studied under the ARPA supported visible laser kinetics program at AERL involves the atomic lead system. It was initially chosen for study because it had been made to lase on a number of interesting visible wavelength transitions (see Fig. 5) in a high temperature, electric discharge laser configuration. These transitions share a common feature, namely that of terminating on low-lying, optically metastable electronic states. If a volumetrically scalable technique could be utilized to quench these lower laser levels efficiently and selectively, a lead laser could in principle be scaled to large volumes and high power. One method to efficiently remove these low-lying levels involves homogeneous gas phase bimolecular collisional relaxation processes. It was anticipated that a number of quenching gases would be found to relax these states allowing rapid laser pulsing or perhaps CW operation. The laser concept that was suggested was the so-called mercury-lead laser operating on the 4058 Å transition (see Fig. 6). In this scheme, lead would be pumped to the resonance 6p 7s $^3P_1^o$ state by energy transfer processes involving excited states of mercury produced in an electric discharge. Under ARPA Contract DAAH01-72-C-0495, room temperature measurements were performed on the quenching of lead ($^3P_2$) and ($^3P_1$) states by Ar, Xe, H_2, D_2, N_2 and O_2. These experiments identified a number of efficient quenching gases and thereby gave continued support for this prototypical laser concept. To further assess its viability, additional information

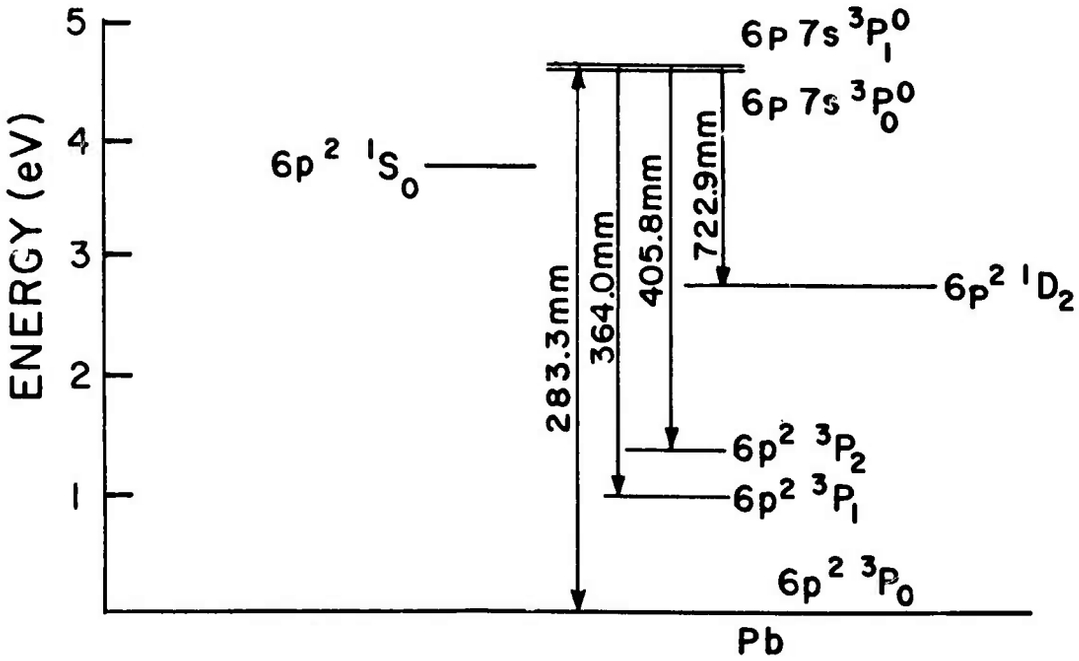

E6994

Fig. 5 Simplified Energy Level Diagram of Lead

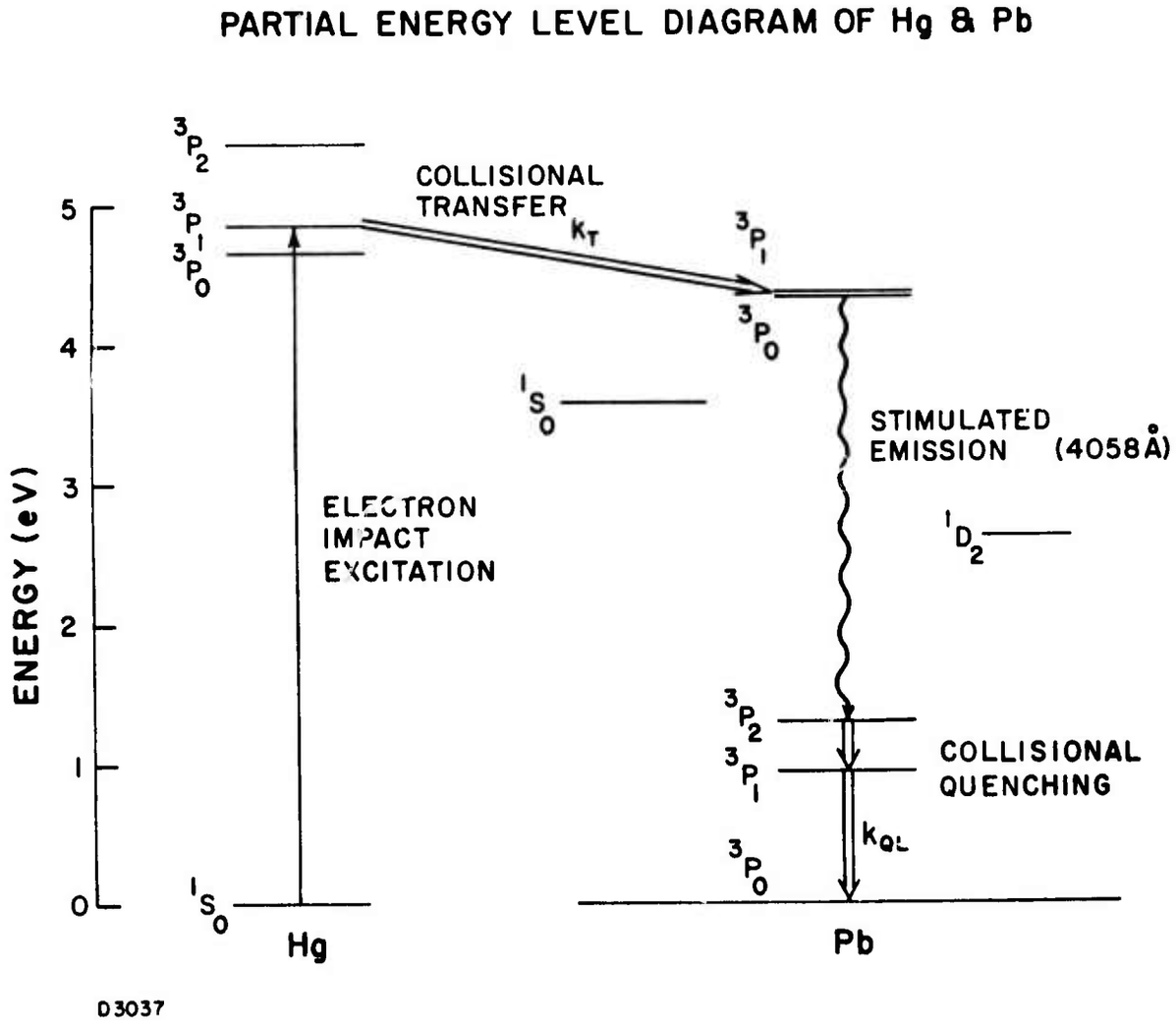

Fig. 6 Mercury-Lead Energy Transfer Laser Concept Operating on the 4058 Å Transition in Lead

was needed, namely: (1) what effect would these identified, efficient quenchers have on the upper laser levels of this 4058 Å transition, i.e., the lead $^3P_1^o$ state? (2) How did these room temperature results scale to higher, more practical operating temperatures characteristic of actual metal vapor lasers? (3) Would mercury, added as a donor specie in the energy transfer scheme, serve a dual purpose and efficiently deactive the lower laser levels? The results of our study to provide information for these important processes were presented in detail in Tasks I and II of this report. These results are also summarized for convenience in Table I. Included in this table with the AERL results are the room temperature results of Husain and co-workers for quenching of the higher lying $^1S_0$ and $^1D_2$ metastable states.

A number of interesting laser possibilities emerge from our combined kinetic picture of the lead system. With regard to the originally proposed mercury-lead laser concept, these are: (1) a number of quenchers are identified which efficiently quench the lower level – the $^3P_2$ state (H_2, D_2, CO_2, etc.). (2) Of these quenching gases only H_2 and D_2 are selective, i.e., they efficiently quench the $6p^2\ ^3P_2$ state but are less efficient in deactivating the upper 6p 7s $^3P_1^o$ level. (3) The original proposal of using Hg ($^3P_0$) as a source of excitation is not viable because: (a) mercury, which was anticipated to be an efficient deactivator of the Pb ($^3P_2$) state is not an efficient quencher; (b) only H_2 and D_2 are efficient and selective with regard to lead and these gases are not compatible with the excited mercury since they quench it at a near gas kinetic rate.

In addition to this allowed 4058 Å transition, these data suggested a new lead laser concept - lead forbidden transition lasers. These lasers

TABLE I

SELECTED PROPERTIES OF THE LOW LYING STATES OF PB ATOMS

Electronic Configuration						
State	$^3P_1$	$^3P_2$	$^1D_2$	$^1S_0$	$^3P_0^o$	$^3P_1^o$
Energy (eV)	0.97	1.32	2.66	3.65	4.31	4.33
Radiative Lifetimes (sec)	.1	2.6	.04	.01	5(-9)	5(-9)
Collisional Quenching Rate Constants cm^3/sec						
Ar[a]	< 1(-16)	< 1(-16)	-	-	c	< 1(-11)[d, e, c]
Xe[a]	< 1(-16)	< 2(-15)	< 1(-15)[b]	< 2(-15)[b]	c	< 1(-11)[d, e, c]
H_2[a]	2(-15)	2(-12)	< 1(-14)[b]	< 1(-14)[b]	c	< 1.4(-12)[c]
D_2[a]	2(-16)	8(-12)	-	-	c	< 1.7(-12)[c]
N_2[a]	1(-15)	5(-13)	< 1(-15)[b]	2(-15)[b]	c	1.5(-10)[d, e, c]
CO_2[b]	< 1(-14)	2(-11)	< 1(-14)	4(-15)	c	4(-10)[d, e, c]
CH_4[b]	< 2(-15)	2(-11)	< 1(-14)	< 1(-14)	-	6(-10)[c]
CF_4[b]	< 4(-15)	3(-11)	< 1(-14)	< 5(-16)	-	1(-9)[c]
SF_6[b]	2(-15)	2(-13)	< 1(-15)	2(-15)	-	> 1(-9)[c]

The notation 5(-9) means 5×10^{-9}.

a. From J. J. Ewing, D. W. Trainor and S. Yatsiv, J Chem. Phys. 61, 4433 (1974).

The temperature dependence of these rates has been recently measured.

D. W. Trainor and J. J. Ewing, Paper #105, 169th ACS National Meeting, Philadelphia, April 1975, J. Chem. Phys. 64, 222 (1976)..

b. D. Husain and J. G. F. Littler, Int. J. Chem. Kinet. 6, 61 (1974), and references therein.

c A. Mandl, Hao-Lin Chen, Phys. Rev., to be published.

d H. M. Gibbs, Phys. Rev. A 5, 2408 (1972).

e. D. R. Jenkins, Proc. Roy. Soc. A 313 (1969).

would operate between the slowly quenched $^1S_0$ and $^1D_2$ states and the rapidly quenched $^3P_2$ state; these forbidden transitions occur at 5314 Å and 9252 Å, respectively with characteristic lifetimes ~0.02 sec (see Table I). Due to these very low transition rates, such lasers are in principle capable of storing high energy densities for extraction in short pulses. These lasers are attractive because the quenching rates, although still required to be selective, can be quite slow due to the long intrinsic lifetime of the laser transition.

Continued research in the atomic lead system should center on identifying efficient excitation schemes for producing the necessary upper state populations for practical laser operation. These schemes may involve direct electron impact excitation (i.e., discharge pumping) or indirect techniques utilizing energy transfer processes.

APPENDIX A

TEMPERATURE DEPENDENCE OF THE SPIN-ORBIT RELAXATION OF LEAD, $6p^2$ ($^3P_2$) AND ($^3P_1$)

Daniel W. Trainor and J. J. Ewing
Avco Everett Research Laboratory, Inc.
Everett, Ma. 02149

ABSTRACT

Rate constants for the collisional deactivation of Pb $6p^2$ ($^3P_2$) and ($^3P_1$) metastable states are reported over the temperature range 300 to 600°K. Quenching data over this temperature range were obtained for relaxation by Ar, Xe, H_2, D_2, N_2 and by Hg at 373°K. These results were obtained in a temperature controlled, flash photolysis apparatus using tetramethyl lead as a precusor and time resolved atomic resonance absorption techniques for monitoring the $^3P_2$ and $^3P_1$ metastable states of interest.

I. INTRODUCTION

The collisional relaxation of electronically excited metastable states of atoms has received considerable experimental study.[A-1] Almost all of the low lying states of non-transition elements have been the subject of some measurements of the kinetics of collisional relaxation. Included are measurements on species like Hg $6p\ ^3P_0$ in which the electronic metastable state has a different configuration than the ground state of the atom;[A-2] $O\ ^1D$, where the metastable state has the same configuration as the ground state but differs in orbital angular momentum;[A-3] and states such as the $6p^2\ ^3P_{2,1}$ states of Pb[A-4, A-5] which are split from the ground state by spin orbit interactions. Although many room temperature measurements have been made, few measurements of the temperature dependence of such relaxation phenomena have been obtained. Exceptions include the temperature dependence of spin orbit relaxation of $I\ ^2P_{1/2}$[A-6] and $Tl\ ^2P_{3/2}$,[A-7, A-8] although the two temperature measurements for Tl were not obtained by the same workers. Quenching of $As\ ^2D_J$[A-9] has also been studied over a limited temperature range. This paper reports the temperature dependence of the kinetics of relaxation of the Pb $6p^2\ (^3P_{2,1})$ states by Ar, Xe, N_2, D_2 and H_2 over the temperature range 300-560°K and the relaxation by Hg at 373°K. All of the data were obtained using a temperature controlled flash photolysis, kinetic spectroscopy apparatus which is a modification of the apparatus used to make room temperature measurements on these metastable lead states.[A-4]

Temperature dependent rate data naturally provide tests of theories describing the underlying physics and chemistry by which collisional removal of such states take place. Collisional deactivation can occur by a number of mechanisms: curve crossings, chemical reactions, E→E (electronic to electronic) and E→V (electronic to vibrational) energy transfer processes, etc., each of which can have various temperature dependences determined by the detailed nature of the potential surfaces and coupling operators. Such mechanisms are usually suggested by the magnitudes of the measured rate constants, inspection of the energy levels of the reactants, and plausible arguments based on the relative magnitude of the quenching rate one could expect for any given energy mismatch. Measurements of the product channels are scarce. For example, E→V energy transfer has been offered as the principal deactivation mechanism for a variety of systems but direct proof has only been obtained for a few systems.[A-10, A-11, A-12] Since the disappearance of a particular metastable state population is the usual diagnostic, it is not trivial to prove any such mechanism. For those systems where monitoring the internal state distribution of products is difficult or impractical, for example in the E→V process when the quenching gas is a homonuclear diatomic molecule, comparison of a plausible model to rate data taken at several temperatures would be advantageous.

Previous room temperature experimental determinations[A-4, A-5] of quenching rate constants for Pb $^3P_2$ by D_2, H_2 and N_2 show that all three molecules relax this excited state with fairly large cross sections at room temperature. It is reasonable to interpret these fast rates in

terms of an E→V process with $^3P_2$ relaxing to $^3P_1$; such an E→V process with $\Delta V=+1$ is very nearly resonant for D_2 though not nearly resonant for N_2 and H_2. The E→V process with N_2 is slightly exothermic whereas in H_2 the energy transfer would be endothermic. Naively, one might expect different temperature dependences to be operative for each of these cases.

A simple model calculation for the quenching cross sections of Pb $^3P_2$ by D_2 has been given.[A-13] This particular case is a good example of metastable relaxation which can occur by a very nearly resonant E→V energy transfer process. The transition D_2 (v=0, J=2) → D_2 (v=1, J=0) is only 18 cm^{-1} off resonance from the infinite separation splitting of the Pb $^3P_2$ and $^3P_1$ states. This is a quadrupole allowed transition, and for temperatures near room temperature roughly 40% of the D_2 molecules are in J=2. The coupling of initial and final states in such a near resonant process could occur by virtue of long range attractive forces.[A-13] Analogous V→V, R near resonant processes have received substantial theoretical analysis.[A-14, A-15] As in the case of near resonant V→V energy transfer, such a nearly resonant E→V process is predicted to show a negative temperature dependence. In an analogous E→R energy transfer, the relaxation of Cs 6 $^2P_{3/2}$ to $^2P_{1/2}$ by CH_4 appears to show such a negative temperature dependence[A-16] in agreement with the predictions of a long range forces model.

II. EXPERIMENTAL

The apparatus, schematically shown in Fig. A-1, was similar to that described in earlier publications. The following modifications were made: (1) Nichrome heating wire (0.0126 in. diameter) was wound in a spiral over the entire surface of the reaction cell at approximately 8 mm intervals; (2) the reaction cell and flashlamps were enclosed in an insulated box to which two 1000 W electric heat guns were attached; (3) the quartz windows of the cell were fused to the cell itself, whereas the previous system used an epoxy seal. In the cell, temperatures in excess of 600°K were easily obtained as determined by three thermocouples (Iron-Constantan) placed at various locations on the glassware surface. The capability of heating this system to high temperatures allowed us to very effectively de-gas the photolysis cell (residual pressures of 10^{-5} Torr, and leak plus outgassing rate of less than 0.1 μ/min).

The overall procedure was the same as that used in the previous room temperature experiments. Premixed gases were introduced into the evacuated reaction chamber. Nonequilibrium concentrations of the $^3P_2$ and $^3P_1$ states of lead were generated by the flash photolysis of a trace amount of tetramethyl lead (TML) in the presence of a buffer gas (Ar) and added quenchers. The decay of the nonequilibrium populations in the $^3P_2$ and $^3P_1$ states was monitored by time resolved line absorption techniques at 4058 and 3683 Å respectively, beginning at times typically 100 μsec after the photolysis flash. The light source was a water cooled

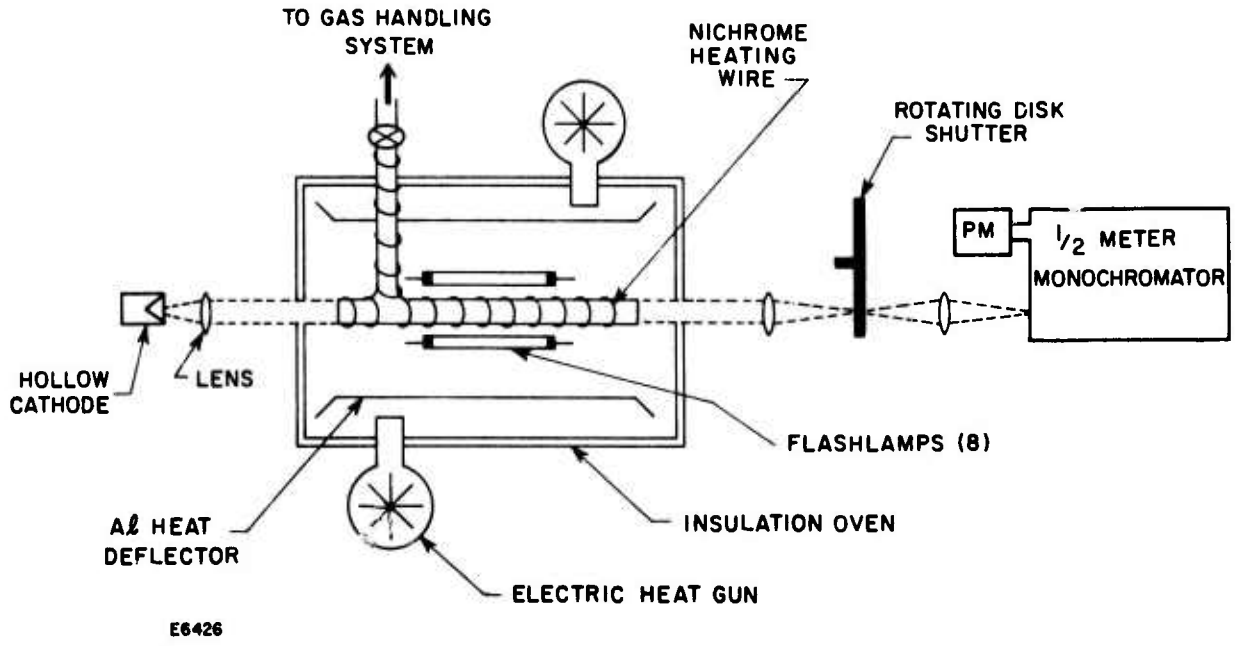

Fig. A-1 Schematic Diagram of Apparatus

Pb hollow cathode lamp (Barnes Engineering). The lamp intensity monitored by a photomultiplier (1 P28) mounted on a 1/2 m monochromator whose output voltage was displayed on an oscilloscope for photographic recording. The usual modified Beer-Lambert Law was used with $\gamma = 1$ as determined by a previous investigation.[A-17] The system was baked under vacuum at a temperature higher than the highest one used for kinetic measurements. Rate constants were first determined at room temperature for each quenching gas to establish that the results were in agreement with our previous work. The system was then heated, premixed gases admitted to the hot cell and measurements made at temperatures up to 600°K.

Extension of these measurements to temperatures > 600°K was hampered by the finite rate of thermal decomposition of the TML at high temperature.[A-18] Decomposition of the TML restricted the residence time of the gases in the cell. For our non-flowing apparatus, the residence times were limited to about two minutes, more than sufficient time for thermal equilibration within the cell but too short a time for significant TML decomposition. For the case of rate studies in which the quenching gas was mercury, completely premixed gases could not be employed because of the low Hg vapor pressure at room temperature. For these experiments, Hg vapor was first admitted to the evacuated cell from a variable temperature heat bath whose temperature was selected to attain the desired vapor pressure of Hg. Hg reservoir temperatures in the range of 90 to 100°C were used to vary the Hg vapor pressure from about 0.15 to 0.3 Torr. The Hg vapor was allowed to flow from the reservoir through a short addition arm maintained at elevated temperatures into the evacuated cell for about two minutes. A premixed 50 Torr mixture of Ar

containing 1 ppm of TML was then slowly added to the Hg vapor. After waiting two minutes to accomplish reasonable mixing,[A-19] the experiments were initiated by discharging the capacitors to photolyze the TML.

Cylinder gases that were used directly include: Ar (liquid Carbonic, 99.998%), Xe (Matheson, Research Grade), H_2 (Matheson, 99.95%), and D_2 (Matheson, 99.5%). Due to a discrepancy between our previous room temperature results[A-4] and that of Husain and Littler[A-5] for quenching of $^3P_2$ by N_2, the nitrogen was further purified by passing the cylinder gas (Liquid Carbonic 99.996%) through a glass coil trap cooled to 77°K. The Hg (Howe and French, Boston, Ma., triple distilled) was also further purified by additional distillation under a high vacuum and then sealed under vacuum in an all welded stainless steel sample cell with a metal bellows valve. The Hg cell was connected to the flash apparatus through a graded glass to metal seal.

III. RESULTS

In the absence of secondary feeding reactions from higher lying states, the decay after the flash of a particular lead excited state, Pb^*, is governed by

$$\frac{-d\,[Pb^*]}{dt} = \tau_{OBS}^{-1}\,[Pb^*]$$

where τ_{OBS}^{-1} is the observed pseudo first order rate constant as determined from the slope of a plot of $\ell n\ \ell n\ [I_o/I(t)]$ vs time.[A-4] The observed decay time is due to collisional deactivation processes involving the added quencher, Q, the Ar buffer gas, and TML and its photofragments, impurities, etc., labelled N_i. Wall reactions are unimportant on our time scale. The observed decay frequency is then given by

$$\tau_{OBS}^{-1} = k_Q\,[Q] + k_{Ar}\,[Ar] + \sum_i k_i\,[N_i]$$

By performing a sequence of experiments in which the TML and Ar (and thus impurity) concentrations are fixed and varying amounts of quencher Q have been added, the rate constant is readily determined by a plot of τ_{OBS}^{-1} vs Q. Such experiments were performed for the gases Ar, Xe, N_2, D_2 and H_2 with results obtained at 298, 500, and 560°K. The Hg experiments were performed at T = 373°K. Typical plots of the decay frequency of Pb $^3P_2$ as a function of added H_2 pressure at these temperatures are shown in Fig. A-2, A-3, and A-4. Note that the zero quencher density intercept of these plots is a function of temperature at fixed buffer gas pressure. This is due to the decrease in buffer gas density

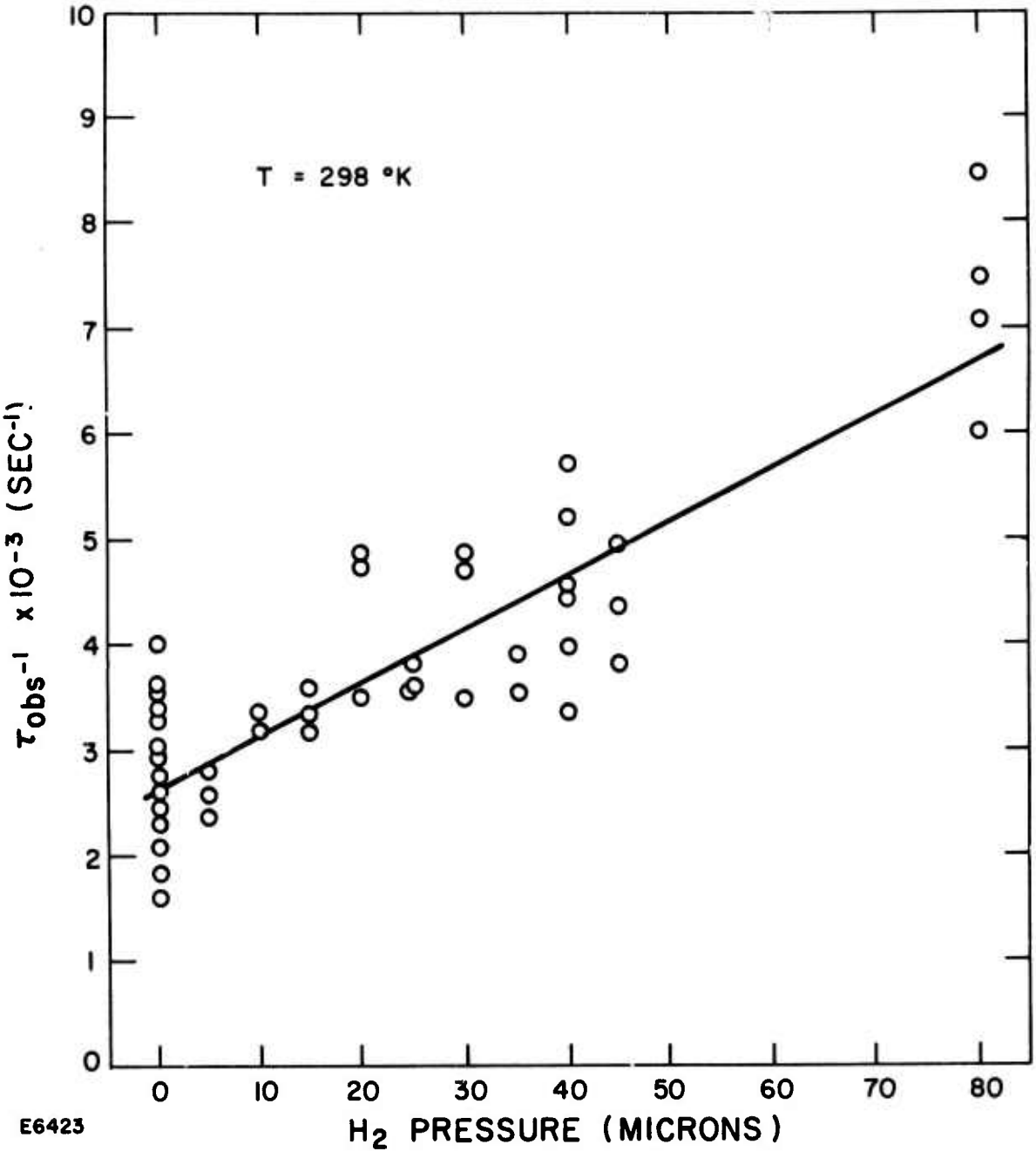

Fig. A-2 Plot of Pseudo First Order Rate Constant τ_{OBS}^{-1} vs P_{H_2} at 298°K for Pb $^3P_2$ monitored 4058 Å

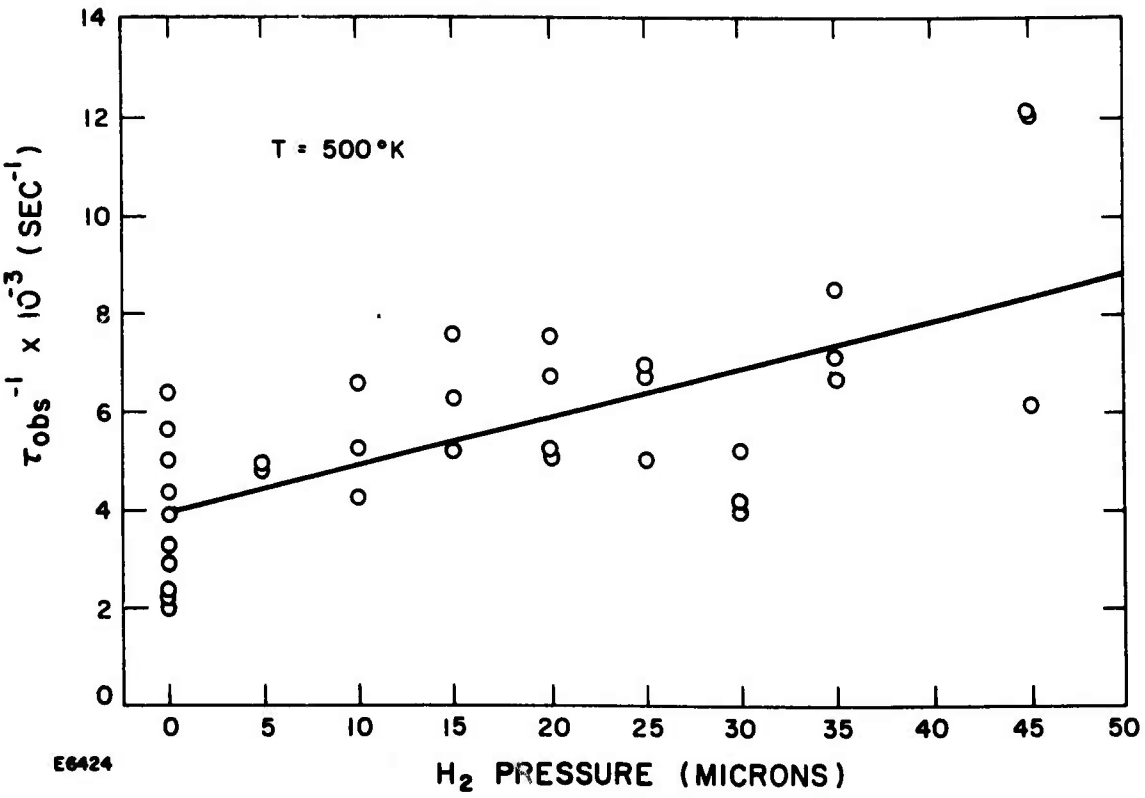

Fig. A-3 Plot of Pseudo First Order Rate Constant τ_{OBS}^{-1} vs P_{H_2} at 500°K for Pb $^3P_2$ monitored 4058 Å

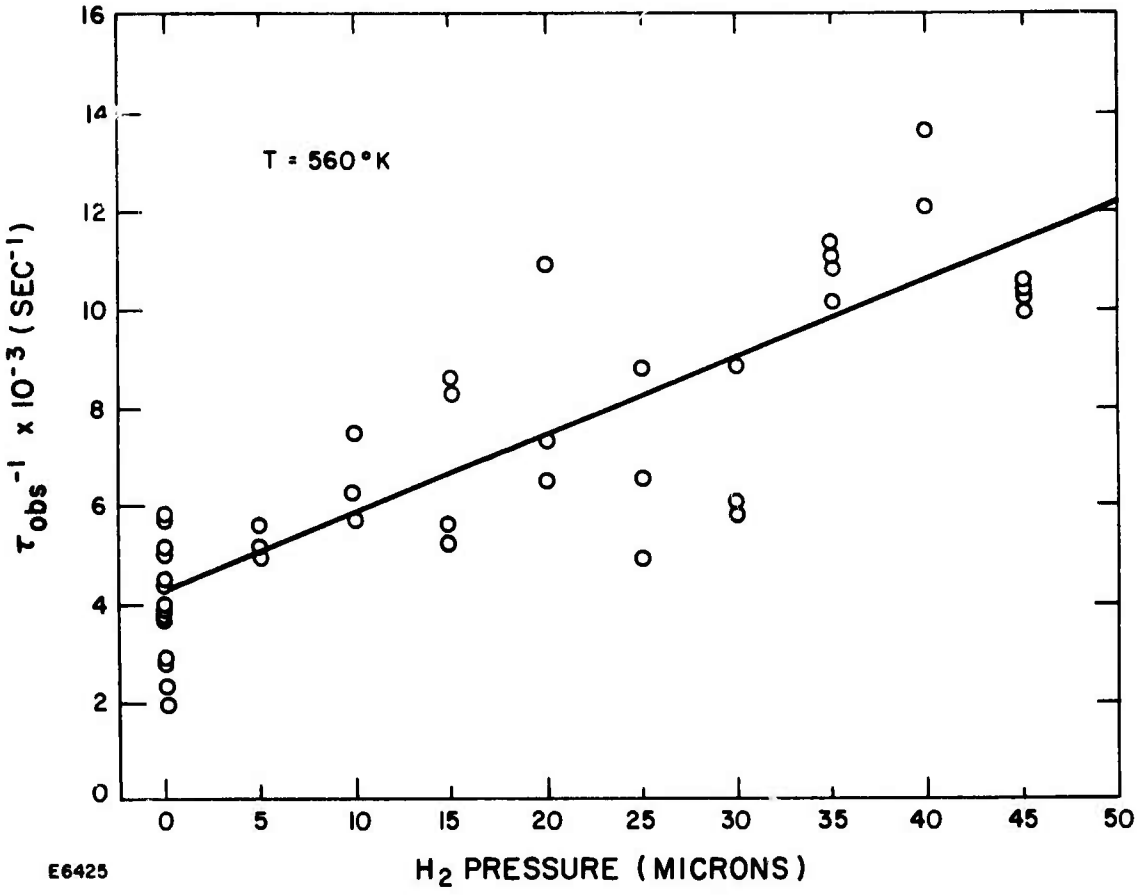

Fig. A-4 Plot of Pseudo First Order Rate Constant τ_{OBS}^{-1} vs P_{H_2} at 560°K for Pb $^3P_2$ monitored 4058 Å

at higher temperatures and the small temperature dependence for quenching by TML, Ar, and the impurities. Similar plots were generated for the other quenchers for both the $^3P_2$ and $^3P_1$ states. These data are summarized in Table A-1. Where uncertainties are indicated, they represent one standard deviation of a least square computer fit to the data.

Rate constants are reported as upper bounds for two distinct classes of results. First, when the ratio of the derived rate constant to the gas kinetic rate is less than the mole fraction of impurities in the quenching gas, the rate is given as an upper bound because of our uncertainty in assigning the observed increase in τ_{OBS}^{-1} to the quencher under investigation or to the impurities which come with the quencher. These bounds appears primarily for inert gas quenching of both states and molecular quenching of the $^3P_1$ state. A different kind of bound is reported for Pb ($^3P_1$) and ($^3P_2$) quenching by Hg at 373°K. In this instance, no change in τ_{OBS}^{-1} with increasing Hg densities could be observed for the range of concentrations of Hg that we used.

These results can be fit to an Arrhenius expression, i. e., $k = A \exp(-Eact/RT)$. Table A-2 summarizes the Arrhenius parameters for those cases where the results are not reported as bounds. The error limits for these parameters were estimated from the maximum and minimum values for the slopes and intercepts which could be drawn and be consistent with the data.[A-20] In general, little temperature variation of the rate constants was observed.

The present data at 298°K, summarized in Table A-1, are in excellent agreement with our prior room temperature results[A-4] and with the work of Husain and Littler.[A-5] There are two exceptions,

TABLE A-1

SUMMARY OF KINETIC RATE CONSTANTS

Reaction	k (cm^3/sec)		
	298°K	500°K	560°K
$^3P_1$ + Ar	$<1.7 \pm 0.4 \times 10^{-16}$	$<2.1 \pm 0.3 \times 10^{-16}$	$<2.6 \pm 0.5 \times 10^{-16}$
+ Xe	$<1 \times 10^{-16}$		
+ N_2	$<8.5 \pm 0.6 \times 10^{-16}$	$<9.4 \pm 0.8 \times 10^{-16}$	$<7.9 \pm 1.0 \times 10^{-16}$
+ D_2	$<2.6 \pm 1.5 \times 10^{-16}$	$<8.6 \pm 1.5 \times 10^{-16}$	$<5.5 \pm 1.4 \times 10^{-16}$
+ H_2	$1.5 \pm 0.3 \times 10^{-15}$	$8.7 \pm 0.5 \times 10^{-15}$	$1.3 \pm 0.1 \times 10^{-14}$
$^3P_2$ + Ar	$<2.4 \pm 0.9 \times 10^{-15}$	$<4.2 \pm 1.5 \times 10^{-15}$	$<4.4 \pm 1.1 \times 10^{-15}$
+ Xe	$<3 \times 10^{-15}$		
+ N_2	$3.5 \pm 1.3 \times 10^{-13}$	$10 \pm 2 \times 10^{-13}$	$9.0 \pm 2.1 \times 10^{-13}$
+ D_2	$7.7 \pm 0.5 \times 10^{-12}$	$14 \pm 2 \times 10^{-12}$	$14 \pm 1.4 \times 10^{-12}$
+ H_2	$1.6 \pm 0.2 \times 10^{-12}$	$5.8 \pm 1.0 \times 10^{-12}$	$9.2 \pm 0.8 \times 10^{-12}$
$^3P_1$ + Hg	$k \leq 1.5^{+4}_{-1.3} \times 10^{-14}$ cm^3/sec (373°K)		
$^3P_2$ + Hg	$k \leq 1.6^{+4}_{-1.6} \times 10^{-14}$ cm^3/sec (373°K)		

TABLE A-2

KINETIC RATE CONSTANTS

(Arrhenius Parameters)

Reaction	A (cm^3/sec)	E_A (kcal)
$^3P_1 + H_2 \rightarrow$	$1.3 \pm 0.3 \times 10^{-13}$	2.7 ± 0.2
$^3P_2 + H_2 \rightarrow$	$5.7 \pm 0.9 \times 10^{-11}$	2.1 ± 0.2
$^3P_2 + D_2 \rightarrow$	$2.9 \pm 0.7 \times 10^{-11}$	0.8 ± 0.2
$^3P_2 + N_2 \rightarrow$	$3.4 \pm 2.6 \times 10^{-12}$	1.3 ± 0.6

however. First, the room temperature results for $^3P_2$ quenching by N_2 do not agree with the results of Husian and Littler[A-5]; our currently measured rate constant is larger by about a factor of 50 and essentially unchanged from our earlier work.[A-4] A discussion of this discrepancy is contained in our earlier paper.

The rate constant for deactivation of $^3P_2$ by Xe, reported previously to be 2.3×10^{-13} cm^3/sec,[A-4] is now found to be $<3 \times 10^{-15}$ cm^3/sec. The difference in rate constants is probably due to a trace impurity introduced with the xenon in the previous measurements. We feel, but cannot prove, that the culprit is H_2O vapor which might have been present in our xenon gas addition line and subsequently introduced at the time the Xe experiments were performed. Unfortunately, there are no measurements reported for Pb $^3P_2$ quenching by H_2O.[A-4, A-5] It is entirely plausible, however, that H_2O vapor could be a gas kinetic, selective quencher of the $^3P_2$ state in light of the fact that a number of molecules like CH_4 are selective, efficient quenchers of Pb $^3P_2$ but have a considerably smaller quenching rate constant for Pb $^3P_1$.[A-5] This differential quenching rate for this impurity is necessary since our measurements for $^3P_1$ quenching by Xe show good agreement with our earlier results.

IV. DISCUSSION

For the limited set of species measured here, there are only four combinations of states and quenchers in which a discussion of the temperature dependence of the rate constants is merited: $^3P_2$ relaxation by N_2, H_2 and D_2, and $^3P_1$ relaxation by H_2. The other combinations can only be reported as upper bounds due to the unknown effects of the impurities.

For the quenching of Pb $^3P_2$ by N_2, H_2, and D_2, it is reasonable to assume that these relaxations could be dominated by an E→V energy transfer process in which the Fb is relaxed from $^3P_2$ to $^3P_1$ and the molecules are excited by one vibrational quanta. Neglecting molecular rotations these processes would be: endothermic for H_2 by roughly 1300 cm^{-1}, exothermic for N_2 by roughly 500 cm^{-1}, and slightly endothermic for D_2. The inclusion of D_2 rotational energy shows that there are a number of possible transitions that are essentially near resonances as discussed previously.[A-13] For relaxation of Pb $^3P_1$ by H_2, a $\Delta v = +2$ transition in the molecule would be about 200 cm^{-1} endothermic.

The decay rate constants that we measure are weighted averages of the rate constants specific to each molecular quantum state viz, $k = \Sigma f_J \int \sigma_J(v)\, v\, dv$, where f_J is the fractional probability of an initial molecular quantum state, $\sigma_J(v)$ the cross section for quenching from an initial state of J into all final channels, and v the initial relative velocity of the collision pair. The temperature dependence of the relaxation of Pb $^3P_2$ or $^3P_1$ by a molecule derives then from the variation of f_J with T

and the integral of $\sigma_J(v)$ over the velocity distribution. Our measurements cannot, of course, resolve $\sigma_J(v)$. However, one could start with various models for $\sigma_J(v)$ and, knowing the temperature variation of f_J, calculate $k(T)$ and compare with experiment.[A-21] There is a paucity of theoretical estimates with which to compare. Alternatively, one can look for similarities with other systems to see if there are any trends which could give some assistance to theoreticians.

Table A-3 compares the quenching of Pb $^3P_1$ by H_2 to the only analogous measurements, i.e., those pertaining to I $^2P_{1/2}$[A-6] and Tl $^2P_{3/2}$[A-7, A-8] quenching by H_2. The table lists the A factors, the measured activation energies, and the reaction endothermicity calculated for an assumed E→V process exciting H_2 into $v=2$ with $\Delta J=0$. Three points stand out. The first is that the pre-exponential terms for I and Tl relaxation by H_2 are an order of magnitude larger than that found for Pb. Secondly, even though the I and Tl activation energies seem to scale more or less with the endothermicity, the E_a found for Pb quenching by H_2 is considerably larger than ΔE, especially if one considers molecular rotations for H_2. Thirdly, the pre-exponential factors for all these presumed $\Delta v=+2$ processes listed are considerably smaller than the pre-exponential factors found for the presumed $\Delta v=+1$ transitions listed in Table A-2. Recent theoretical calculations by Zimmerman and George[A-22] for energy transfer in $I^* + H_2$ and $Br^* + H_2$ for an assumed collinear geometry show that the maximum cross section for the $\Delta v=+2$ process in $I^* + H_2$ is about 1/3 of the corresponding peak cross section for the $\Delta v=+1$ transition for $Br^* + H_2$. Also, the quadrupole transition moment

TABLE A-3

COMPARISONS OF ENERGETICALLY SIMILAR SPECIES

Reaction	A (cm^3/sec)	E_A (kcal)	ΔE (kcal)
$Pb\ (^3P_1) + H_2 \rightarrow$	1.3×10^{-13}	2.7	0.7
$I\ (^2P_{1/2}) + H_2 \rightarrow$	2.2×10^{-12}	1.7	1.4
$Tl\ (^2P_{3/2}) + H_2 \rightarrow$	1.9×10^{-12}	0.8	0.7

linking H_2 (v = 0) to H_2 (v = 2) is about 1/10 that pertaining to the $\Delta v = +1$ transition.[A-13] Hence, it is not surprising that the quenching of these states in I, Tl, and Pb should have smaller cross sections if indeed they are E→V processes with $\Delta v = 2$.

The fact that the Pb $^3P_1$ relaxation by H_2 has a smaller pre-exponential factor than the energetically similar I $^2P_{1/2}$ and Tℓ $^2P_{3/2}$ quenching by H_2 may be due to the details of the coupling inducing the transition on the metal atom since the molecular part of the collision is kept fixed. As pointed out in Ref. (A-13), the quadrupole or higher multipole components of the long range forces cannot couple Pb ($^3P_1$) to ($^3P_0$). On the other hand, the $J = 3/2 \rightleftarrows 1/2$ transitions in the I and Tℓ systems are not forbidden to the electric quadrupole interaction. The fact that the activation energy for Pb $^3P_1$ quenching is slightly larger than that pertaining to I and Tℓ is also somewhat puzzling.

In the case of the rapid relaxation of Pb $^3P_2$ by H_2, D_2, and N_2, the results are naturally rationalized in terms of an E→V process in which the molecules are excited by one vibrational quanta. We will discuss our results first for H_2.

There are no similar temperature dependence measurements for a slightly endothermic process involving a $\Delta v = +1$ molecular transition. However, Zimmerman and George[A-22] have done calculations for the analogous Br ($^2P_{1/2,\ 3/2}$)/H_2(v) system using collinear potential surfaces for this system. These calculations clearly show that the probability of transitions from one electronic surface to another by an E→T process such as

$$Br\ (^2P_{1/2}) + H_2\ (v = 0) \rightleftarrows Br\ ^2P_{3/2} + H_2\ (v = 0)$$

have considerably lower probability than the more closely resonant process in which one quanta of H_2 vibration is excited

$$Br\ ^2P_{1/2} + H_2\ (0) \rightarrow Br\ (^2P_{3/2}) + H_2\ (v = 1).$$

The Br E→V mechanism is endothermic by ~ 600 cm^{-1} while that proposed for the Pb $^3P_2$ + H_2 system is endothermic by ~ 1300 cm^{-1}. The Br/H_2 calculations show the cross section for the E→V process turns on near 0.85 eV, an energy somewhat in excess of the total energy needed to open up the E→V channel, and smoothly rises to a maximum probability of about 0.7 near 1.25 eV. This kind of an energy dependence for the cross section would give a rate constant temperature dependence for Pb $^3P_2$ relaxation by H_2 with a pre-exponential factor near gas kinetic and an activation energy of the order of the endothermicity, in general agreement with the experimentally observed data reported here.

For the case of D_2 quenching of $^3P_2$, a number of quadrupole allowed $\Delta v = +1$ transitions in D_2 are resonant with the Pb $^3P_2$, $^3P_1$ splitting.[A-13] Overall, one would then anticipate that the quenching rate should be dominated by contributions due to near resonant processes, induced by the very long range forces of interaction. Such processes can show a negative temperature dependence. The experimentally observed temperature dependence for Pb $^3P_2$ quenching by D_2 shows a <u>positive</u> temperature dependence, however. In addition, the simple theory[A-13] predicts a total cross section larger than observed. These two discrepancies between theory and experiment could derive from various inadequacies in the simple theory given earlier.[A-13] The total cross

section as calculated could have been overestimated if the quadrupole transition matrix elements used for the Pb + D_2 calculation were too large, or the impact parameter too small, or both. Possibly the assumption of the applicability of first order perturbation theory is also invalid. If the contribution due to the long range forces coupling the near resonant channels was overestimated, the influence of its contribution on the total cross section representing all deactivation channels could be reduced and therefore the temperature dependence over this limited range could be determined by other forces, e.g., short range repulsive forces or curve crossings on the combined Pb/D_2 triatomic surface. The qualitative predictions of the long range attractive forces theory[A-13] also do not agree with recent measurements of relative quenching rates for Sn $^3P_1$ and Sn $^3P_2$.[A-23] This also suggests that other coupling mechanisms must be involved.

The quenching of Pb $^3P_2$ by N_2 shows a slight positive dependence on temperature. The measured change in rate constants with temperature is slightly larger than that which would prevail if the average cross section was constant and the rate increase was solely due to the increase in relative velocity. Whereas the H_2 and D_2 pre-exponential factors are within a factor of 2 of each other, the pre-exponential for N_2 is lower by about a factor of 10, which is more than a simple reduced mass factor. We have no explanation for the N_2 temperature dependence.

In summary, we have measured the decay rate constants for Pb ($^3P_2$, $^3P_1$) quenching by a few simple gases. The new room temperature data agrees with previous measurements and these rate constants do not change dramatically with temperature. The largest temperature

dependences are found for systems where the presumed E→V excitation is somewhat endothermic. The observed temperature dependence of Pb $^3P_2$ quenching by D_2 is not what one would expect from a simple near resonant E→V theory.

ACKNOWLEDGMENT

We wish to thank Mr. Anthony Montagna for his contribution to developing this facility and in running the experiment.

APPENDIX A

REFERENCES

A-1. Donovan, R. J. and Husain, D., Chem. Rev. 70, 489 (1970).

A-2. Callear, A. B. and McGurk, J. C., Chem. Soc. Faraday Trans. II 69, 97 (1973).

A-3. Heidner, R. F., III and Husain, D., Int. J. Chem. Kinet. 6, 77 (1974).

A-4. Ewing, J. J., Trainor, D. W. and Yatsiv, S., J. Chem. Phys. 61, 4433 (1974).

A-5. Husain, D. and Littler, J. G. F., Int. J. Chem. Kinet. 6, 61 (1974).

A-6. Deakin, J. J. and Husain, D., Chem. Soc. Faraday Trans. II, 68, 1603 (1972).

A-7. Bellisio, J. A. and Davidovits, P., J. Chem. Phys. 53, 3474 (1970).

A-8. Wiesenfeld, J. R., Chem. Phys. Lett. 21, 517 (1973).

A-9. Callear, A. B. and Oldman, R. S., Trans. Far. Soc. 64, 840 (1968).

A-10. Leone, S. R. and Wodarczyk, F. S., J. Chem. Phys. 60, 314 (1974).

A-11. Karl, G., Kraus, P. and Polanyi, J. C., J. Chem. Phys. 46, 224 (1967).

A-12. Lin, M. C. and Shortridge, R. G., Chem. Phys. Lett. 29, 42 (1974).

A-13. Ewing, J. J., Chem. Phys. Lett. 29, 50 (1974).

A-14. Sharma, R. D. and Brau, C. A., Phys. Rev. Lett. 19, 1273 (1967).

A-15. Sharma, R. D. and Brau, C. A., J. Chem. Phys. 50, 924 (1969).

A-16. Walentynowicz, E., Phaneuf, R. A., Baylis, W. E. and Krause, L., Can. J. Phys. 52, 584 (1974).

A-17. We have previously determined γ to be one at room temperature (Reference A-4) implying a reasonably unreversed source. This information and plausible arguments based on calculated line profiles for these experimental conditions suggest the Lambert-Beer relationship should also hold true for small absorption over this

limited temperature range - (see for example, Bemand, P. B. and Clyne, M. A. A., Chem. Soc. Faraday Trans. II 69, 1643 (1973)). If γ changes with temperature, i. e., $\gamma < 1$, the effect would be that the rate constants reported here would be lower limits, i. e., $k_{true} = k_{observed}/\gamma$.

A-18. Homer, J. B. and Hurle, I. R., Proc. R. Soc. Lond. 327, 61 (1972).

A-19. This two minute time delay was determined by the desire to avoid thermal decomposition of the TML and is in fact likely to be too short for complete mixing to occur at these densities. We calculated the spatial distribution of Hg atoms in the section of the cell where photolysis can occur assuming purely diffusive mixing with a diffusion constant of D = 3.54 cm^2/sec. The calculation showed the Hg density in the region of the cell to be within a factor of two of the completely mixed equilibrium condition. The error limits stated for the Hg rate constants include this uncertainty in knowing the actual Hg density in the cell.

A-20. Shoemaker, D. P. and Garland, C. W., "Experiments in Physical Chemistry," (McGraw-Hill Book Co., New York, 1962), Chap. 2, p. 34.

A-21. Butcher, R. J., Donovan, R. J. and Strain, R. H., Chem. Soc. Faraday Trans. II 70, 1837 (1974).

A-22. Zimmerman, I. H. and George, T. F. (to be published).

A-23. Foo, P. D., Wiesenfeld, J. R. and Husain, D., Chem. Phys. Letters 32, 443 (1975).

APPENDIX B

COLLISIONAL RELAXATION OF ELECTRONICALLY EXCITED COPPER: $3d^9 4s^2 \, (^2D_{5/2})$

Daniel W. Trainor
Avco Everett Research Laboratory, Inc.
Everett, Massachusetts 02149

I. INTRODUCTION

There currently exists a rather extensive collection of rate constant information describing processes whereby optically metastable excited electronic states of atoms are relaxed in collisions with a variety of simple atomic and molecular quenchers. Such data are being collected at an accelerated pace but have largely been confined to room temperature measurements on atoms in groups IVA through VIIA.[B-1] By providing such kinetic information for all members of a given group, the influence of increasing atomic weight on fundamentally similar electronic structures can be characterized and the effects of these changes on observed relaxation data can be correlated with electronic structure and the potential surfaces involved. One group that has received considerable attention in this manner is group VA, (N, P, As, Sb and Bi), notably through the efforts of Husain and coworkers.[B-2] Information on other members of the periodic table, particularly transition elements, is limited; an obvious exception is the large body of quenching data available on Hg(^3P_o).[B-3] With the increasing interest in identifying visible transition lasers, additional kinetic data on metastable states, which have been identified as the lower laser levels of existing or potential visible lasers, of other transition metal atoms would be particularly valuable. One such laser is the 5105.54 Å (green) copper laser terminating on the $3d^9\ 4s^2\ (^2D_{5/2})$ state (see Fig. B-1). Copper lasers operating on this transition have been studied by a number of workers[B-4] and have demonstrated relatively high power (~ 15 watts) and high efficiency (~ 1%).

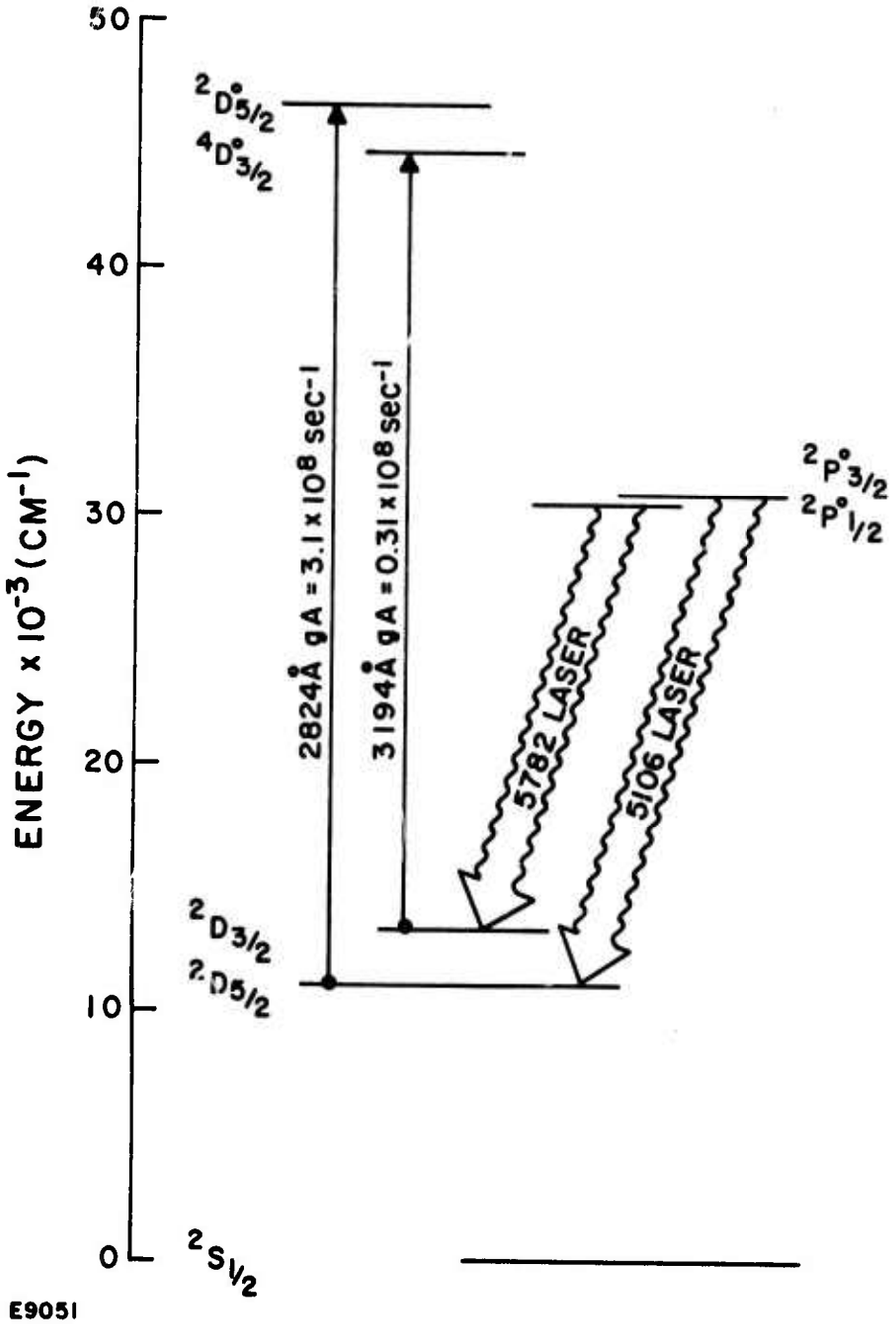

Fig. B-1 Partial Energy Level Diagram for Copper Showing Yellow (5782 Å) and Green (5106 Å) Lasing Transitions and the Resonance Lines Chosen to Monitor the Metastable States Under Investigation

This paper describes a kinetic spectroscopy resonance absorption experiment which provided rate constants for the collisional deactivation of the Cu($^2D_{5/2}$) state by a variety of simple quenching gases. This optically metastable state was produced by the flash photolysis of CuCℓ (or CuI) in a heated reaction vessel (near 600°K) and monitored using time resolved atomic resonance absorption techniques. In addition, an attempt to provide similar information for the $^2D_{3/2}$ state was made, but not direct evidence of any significant production of this state in our flash photolysis apparatus was observed.

II. EXPERIMENTAL

The apparatus and experimental technique has been thoroughly described in earlier publications[B-5-B-7] so only a brief summary will be included here. The apparatus, schematically shown in Fig. B-2, consists of a Glomax hollow cathode light source, a 45 cm long reaction cell (1.8 cm diameter, ID) constructed of suprasil quartz with quartz windows fused to the cell itself, and a mechanical shutter/monochromator/photomultiplier detection system for monitoring the resonance line selected for the time resolved line absorption measurements. In the cell, temperatures in excess of 600°K were easily obtained by resistively heating the Nichrome wire (0.41 mm diameter) which was wound in a spiral over the entire surface of the reaction cell at approximately 3-4 mm intervals. The capability of heating the cell to high temperatures was necessary to obtain significant vapor pressure[B-8] of the copper halides chosen as photolytic precursors of the low lying metastable states. At these temperatures, other studies[B-9] have shown the copper halides exist in the gas phase principally as trimers suggesting multi-photon processes are likely to be occuring during the photodecomposition process. This high temperature capability also allowed us to very effectively de-gas the photolysis cell (residual pressures of 10^{-5} torr, and leak plus outgassing rate of less than 0.1 μ/min).

The overall procedure was the same as that used in the previous experiments[B-7] with one major exception, namely the copper halides are solids at room temperature and, therefore, it was not possible to

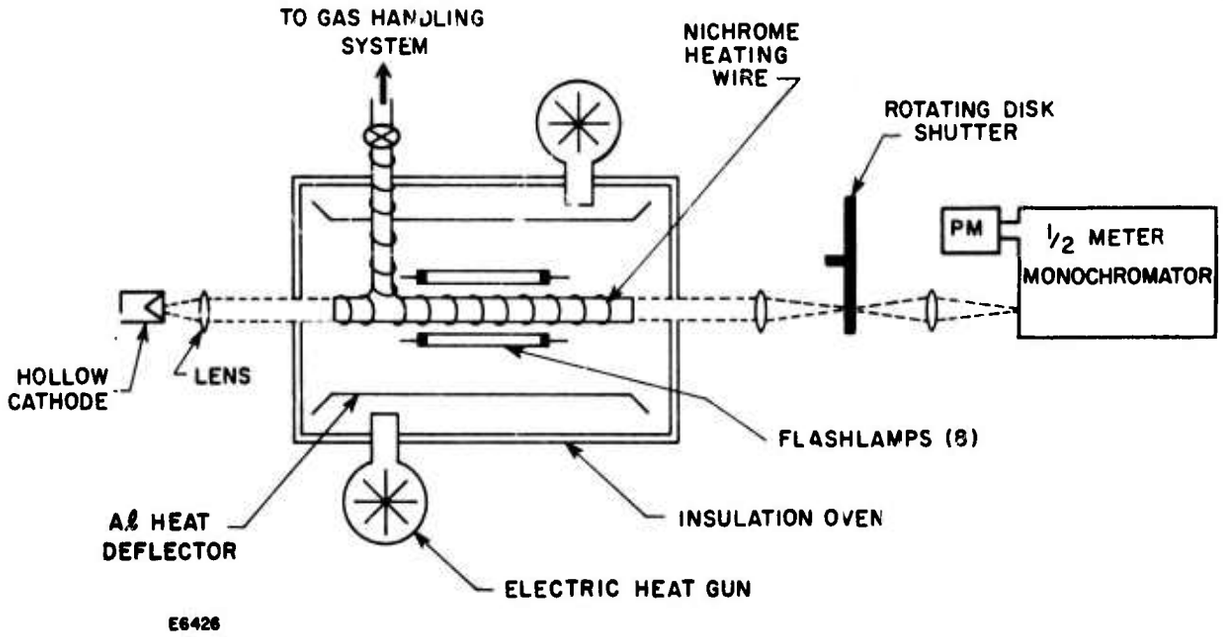

Fig. B-2 Schematic Diagram of the Apparatus

prepare pre-mixed gases containing the precusor of the copper metastable states. Instead, a small quantity of CuX (X = Cℓ or I) was admitted to the cell to act as a reservoir. Since exceedingly small quantities are photodecomposed with each flash, the reservoir provided ample gas phase concentrations for essentially an unlimited number of experiments. To the heated reaction cell containing the CuX, 50 torr of Ar containing varying amounts of quenching gases could be added. Nonequilibrium concentrations of the $Cu\ ^2D_{5/2}$ state were generated by the flash photolysis of the trace amount (typically 0.1 to 1μ pressure calculated based on vapor pressure data[B-8]) of copper halide in the presence of the Ar and added quenchers. The decay of the nonequilibrium population in the $^2D_{5/2}$ state was monitored by time resolved line absorption techniques at 2824Å ($gA = 3.1 \times 10^8\ sec^{-1}$, [B-10] $^2D_{5/2} \leftarrow {}^2D^o_{5/2}$), beginning at times typically 100 μsec after the photolysis flash. In addition, a number of attempts were made to detect photoproduction of the $^2D_{3/2}$ state using resonance absorption at 3194 Å ($gA = 0.31 \times 10^8\ sec^{-1}$, [B-10] $^2D_{3/2} \leftarrow {}^4D^o_{3/2}$) but were inconclusive due to possibly small photoproduction of this state, the relatively weak transition probability for this line, and/or poor signal to noise encountered for our source and detection system for this transition.

The light source was a water cooled copper hollow cathode lamp (Barnes Engineering). The lamp intensity was monitored by a photomultiplier (1P28) mounted on a 1/2 m monochromator whose output voltage was displayed on an oscilloscope for photographic recording. Unfortunately, γ - values[B-11] for the modified Beer-Lambert Law ($I_{TRANSMITTED} = I_o \exp(-\epsilon [C\ell]^\gamma)$) could not be determined. This is a result of the fact that the concentration of precusor could not be varied independently of other

parameters so as to determine the relationships between the intensity of light transmitted and the concentration of metastable copper atoms produced. We have, therefore, assumed $\gamma = 1$ for presentation of these rate constants. This assumption should not cause too serious an error (if any) in these data since for similar conditions, in the same apparatus, for lines of comparable transition probability, we found γ to be essentially 1 for the 4058 Å ($gA = 9.2 \times 10^6$ sec^{-1}, (B-10) $^3P_2 \leftarrow {}^3P_1{}^o$) and 3683 Å ($gA = 3.1 \times 10^8$ sec^{-1}, (B-10) $^3P_1 \leftarrow {}^3P_o{}^o$) transitions in lead.(B-6) For lines of considerably stronger transition probabilities, namely the Bismuth resonance lines: 2898 Å ($gA = 17 \times 10^8$ sec^{-1}, (B-10) $^2D_{3/2} \leftarrow {}^2D_{3/2}$) and 2938 Å ($gA = 61 \times 10^8$ sec^{-1}, (B-10) $^2D_{5/2} \leftarrow {}^2D^o{}_{5/2}$) we found γ to be 0.81 ± 0.11 and 0.87 ± 0.20 respectively.(B-12) The effect of $\gamma < 1$ on the results presented here is that k_{TRUE} (the true bimolecular rate constant) is equal to $k_{OBSERVED}/\gamma$.

Cylinder grade gases were used directly and were of the following purity: Helium (Research Grade, Matheson, 99.9999%) Ar (Liquid Carbonic, 99.998%), Xenon (Research Grade, Matheson, 99.995%) N_2 (Liquid Carbonic, 99.996%), CO (Research Grade, Matheson, 99.99%) CO_2 (Research Grade, Matheson, 99.995) SF_6 (Mass Oxygen Equipment Co., 99.8%) and O_2 (Liquid Carbonic, 99.7%). The Cuprous Chloride (94.1%, Fisher Scientific) and Copper (I) Iodide (Ultrupure, Alfa Products) were subjected to a series of insitu high temperature vacuum despositions as a means of additional purification prior to any experimentation. This was accomplished by subjecting the CuX in the reaction cell to localized high temperature conditions causing the resulting vapor to redeposit in a colder section of the quartz cell. This procedure was then repeated a number of times.

III. RESULTS AND DISCUSSION

The decay of the $^2D_{5/2}$ state of copper, Cu^*, after the flash can be described on the basis of pseudo first order kinetics

$$\frac{-d[Cu^*]}{dt} = k'_{OBS}\,[Cu^*]$$

where k'_{OBS} is defined as the slope of a plot of $\ell n \ell n [I_o/I(t)]$ vs time.(B-6) The observed kinetic behavior is due to collisional deactivation of Cu^* by the copper halide photolytic precusor and its photofragments, the Ar gas added as a buffer, and the system and gas impurities, etc. labelled $[N_i]$. Wall reactions and radiative decay processes are unimportant on our time scale. By performing a sequence of experiments in which the temperature (i.e. copper halide concentration) and buffer concentration are fixed and varying amounts of quenching gas are added, a bimolecular rate constant for the added quencher can be determined from a plot of k'_{OBS} vs $[Q]$, e.g.

$$k'_{OBS} = k_{Ar}\,[Ar] + \sum_i k_i\,[N_i] + k_q[Q]$$

Figure B-3 contains oscillograms showing typical Cu relaxation data for the $^2D_{5/2}$ state being quenched with and without added oxygen. The first order decay plots for these data are shown in Fig. B-4. Similar data for varying concentrations of quenching gases were collected for a number of quenchers and such data were used to construct k'_{OBS} vs $[Q]$ plots.

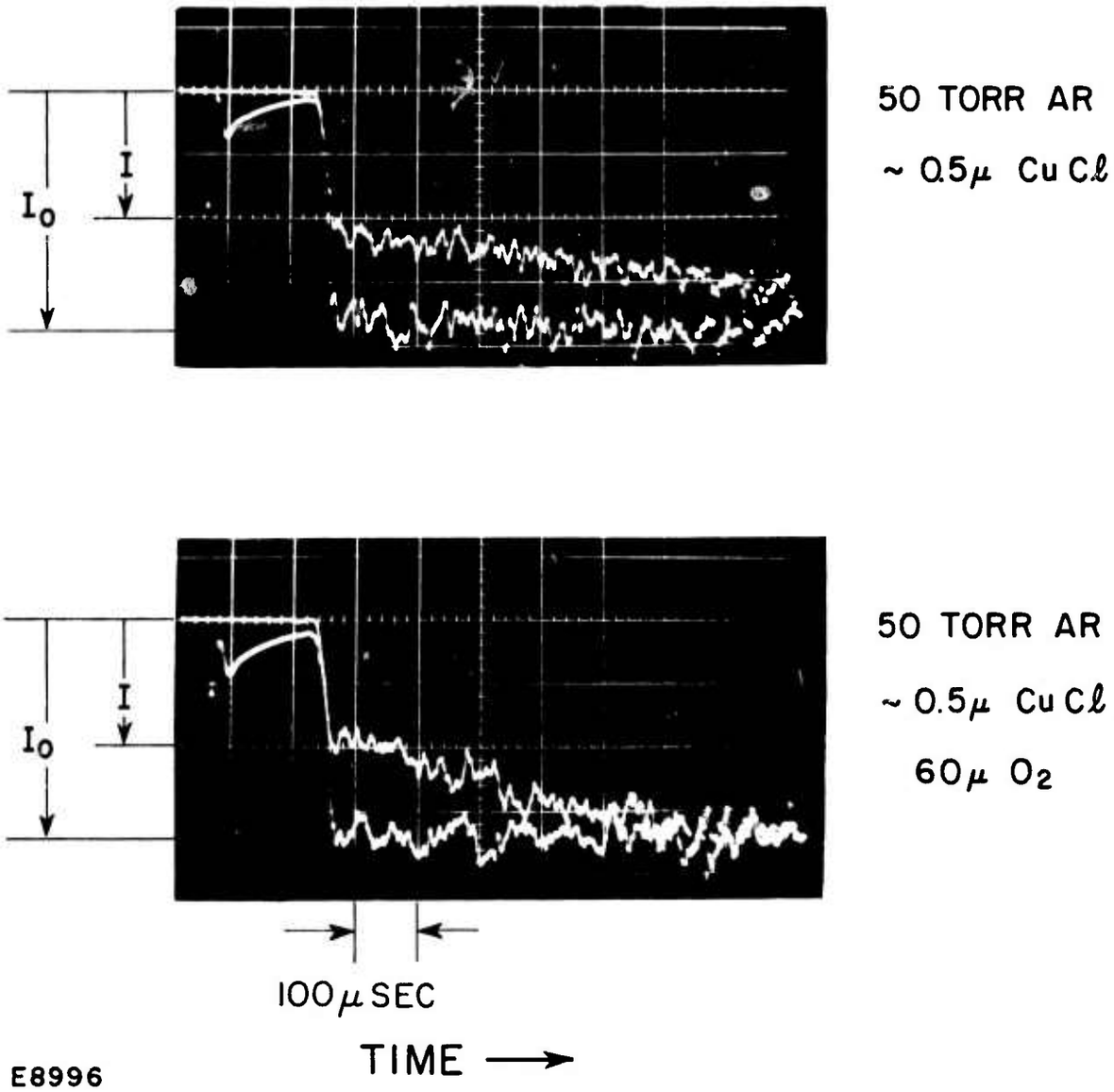

Fig. B-3 Decay of $^2D_{5/2}$ Copper Atoms Monitored at 2824 Å

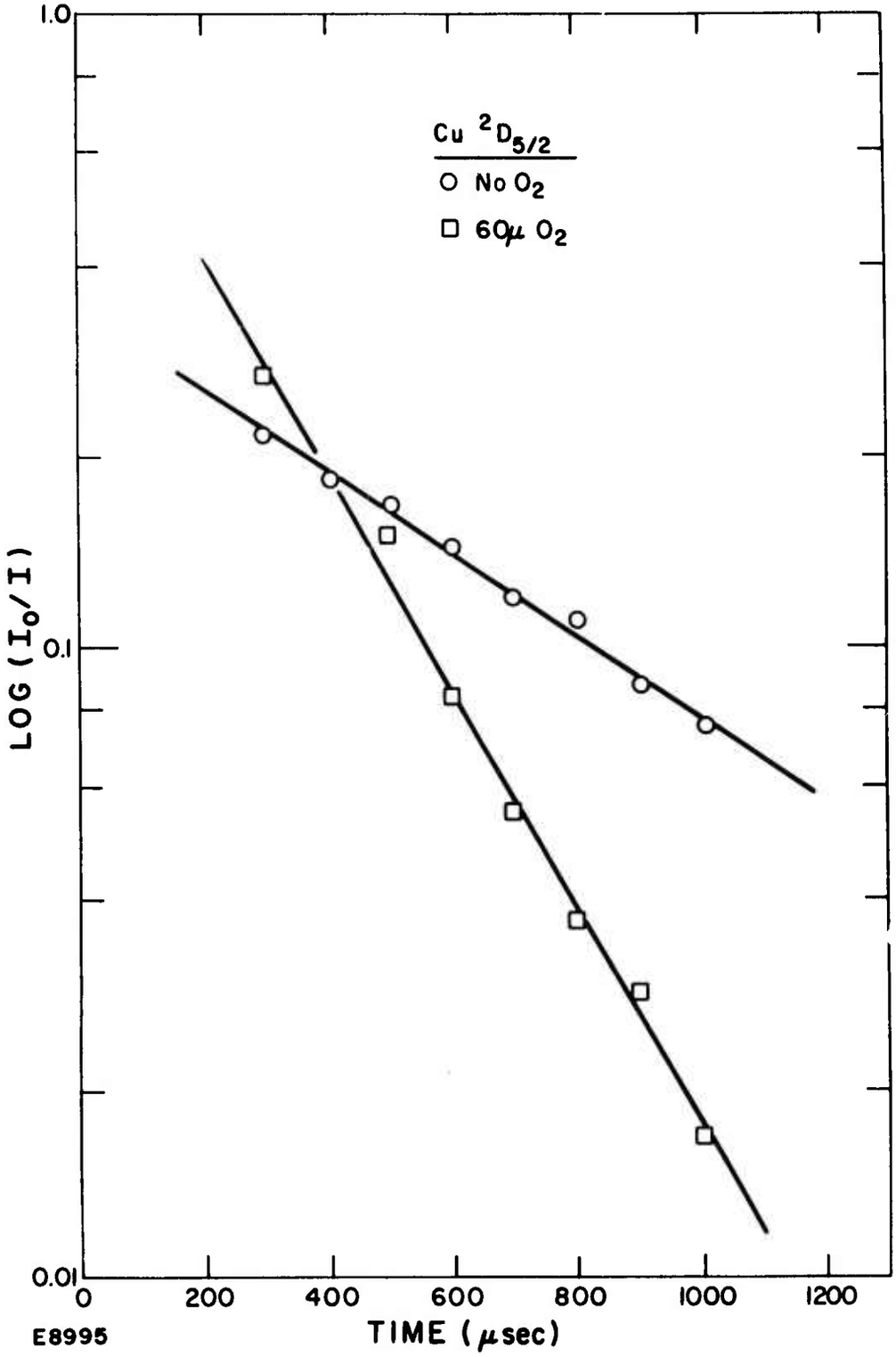

Fig. B-4 Log (I_o/I) vs Time Plot for Data of Fig. 3

From these plots the desired bimolecular quenching rate constants were obtained. A typical example of such a plot is shown in Fig. B-5. Data were obtained with copper chloride as the precursor at 560°K for O_2, and SF_6. With copper iodide as precursor, data were obtained for O_2, SF_6, He, Ar, Xe, N_2, CO, and CO_2 at temperatures near 615°K. The bimolecular rate constants obtained from such plots are summarized in Table B-1. Where uncertainties are indicated, they represent one standard deviation of a least square computer fit to the data.

Rate constants are reported as upper bounds for most of the quenching gases studied. These bounds arise when the ratio of the observed rate constant to a gas kinetic rate constant ($\sim 2 \times 10^{-10}$ cm^3/sec) is less than the mole fraction of impurities in the quenching gas. The rate constant is then listed as an upper bound because of our uncertainty in attributing the observed increase in k'_{OBS}, with increasing quenching gas density, to the quencher under investigation or to the impurities which come with the quenching gas. In general, these quenching gases were inefficient at deactivating this metastable state with the singular exception of molecular oxygen.

With O_2 as the collision partner, the thermochemistry indicates relaxation can occur via chemical reaction

$$Cu\ (^2D_{5/2}) + O_2 \rightarrow CuO + O \quad \Delta H = -37.6 \text{ Kcal}$$

whereas copper in the ground electronic state reacting with O_2 would be endothermic by about 5 kcal.[B-13] Also, simple weak spin orbit coupling approximations show proper symmetry correlations between these reactants and the ground state products.[B-1, B-14]

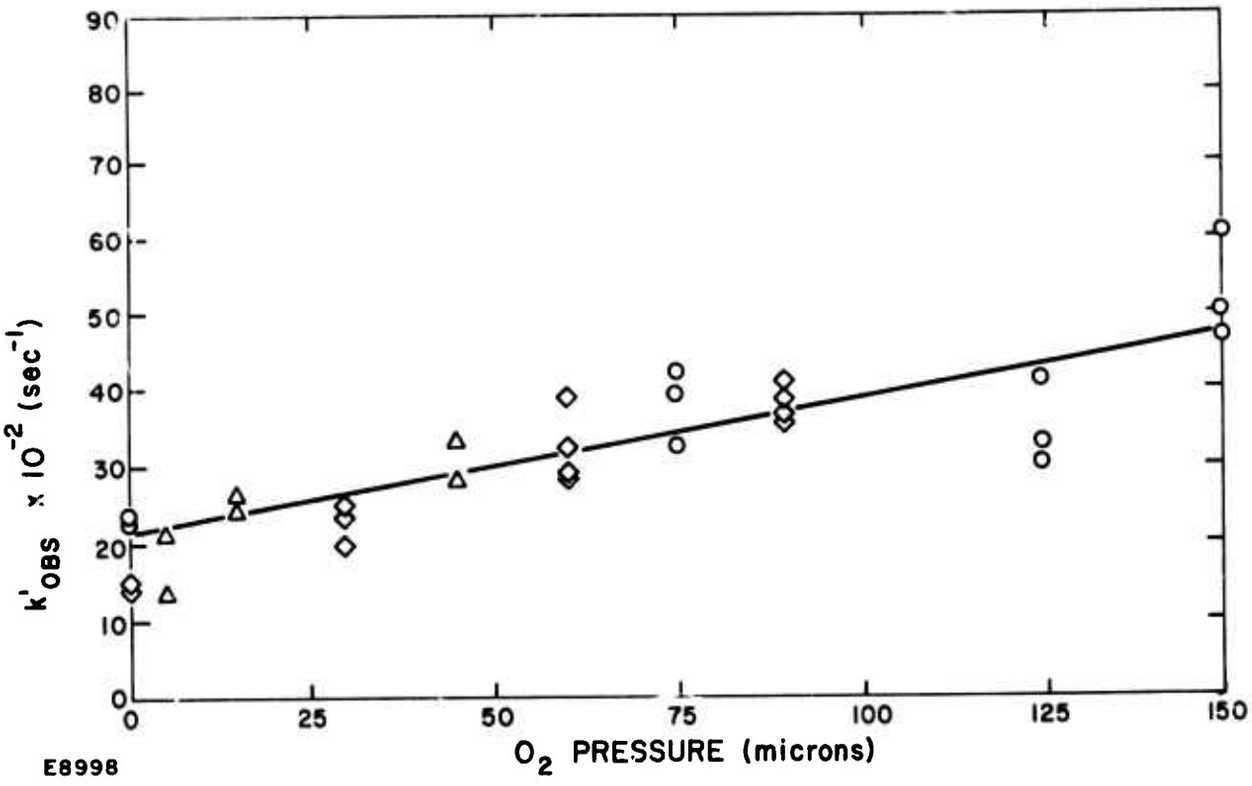

Fig. B-5 Plot of Pseudo-First-Order Rate Constant, k'_{OBS}, vs P_{O_2} at 560°K Using CuCℓ as the Photolytic Precursor and Flash Energy of 600 J

TABLE B-1

COPPER $^2D_{5/2}$ QUENCHING RATE CONSTANTS

REACTION	k (cm^3/sec)	
	(CuI; 615°K; 400 J)	(CuCℓ; 560°K; 600 J)
$Cu(^2D_{5/2})$ + He	$< 5.1 \pm 1.5 \times 10^{-16}$	
+ Ar	$< 1.2 \times 10^{-16}$	
+ Xe	$< 4.7 \pm 1.1 \times 10^{-16}$	
+ N_2	$< 4.9 \pm 1.1 \times 10^{-16}$	
+ CO	$< 5.8 \pm 1.8 \times 10^{-16}$	
+ CO_2	$< 1.1 \, {}^{+1.4}_{-1.1} \times 10^{-16}$	
+ SF_6	$6.4 \pm 1.1 \times 10^{-15}$	$13 \pm 2 \times 10^{-15}$
+ O_2	$3.5 \pm 0.3 \times 10^{-12}$	$1.1 \pm 0.1 \times 10^{-12}$

$$Cu\,(^2D_J) + O_2\,(X^3\Sigma_g^-) \xleftrightarrow{^4A' + {}^4A''} CuO\,(X^2\Sigma^+) + (^3P_J)$$

There appears to be some systematic differences, however, in the results for O_2 (and SF_6) between the data taken at the two temperatures utilized for the two different halide precursors. This difference is likely to be representative of the limited accuracy of these single-shot, high temperature flash photolysis experiments. Certainly agreement between two workers on the same species to a factor of two is considered good agreement.[B-6] It is also possible that there exists some temperature dependent influence on these collisional relaxation process similar to that observed in lead.[B-7] It would be useful to explore this aspect of these results, but it is not practical to do utilizing our experimental approach. The difficulty arises in the correlation between precusor vapor pressure and temperature; any change in temperature causes a corresponding change in the photoproduction of Cu*, and associated photofragments. At higher temperatures, more Cu* may cause deviations from simple Lambert-Beer interpretations, and quenching by photofragments and the CuX compounds would become the dominant loss mechanisms. Conversely, a lowering of temperature causes reduced photoproduction of Cu* and subsequent loss of signal attenuation.

APPENDIX B

REFERENCES

B-1. R.J. Donovan and D. Husain, Chem. Rev. 70, 489 (1970).

B-2. M.J. Bevan and D. Husain, J. Phys. Chem. (to be published) and References Therein.

B-3. J.M. Campbell, S. Penzes, H.S. Sandhu and D.P. Strauss, Int. J. Chem. Kinetics 3, 175 (1971).

B-4. A.A. Isaev, M.A. Kazaryan and G.G. Petrash, JETP Letters 16, 17 (1972).

B-5. S. Yatsiv and J.J. Ewing, Rev. Sci. Instrum. 45, 705 (1974).

B-6. J.J. Ewing, D.W. Trainor and S. Yatsiv, J. Chem. Phys. 61, 4433 (1974).

B-7. D.W. Trainor and J.J. Ewing, J. Chem. Phys. 64, 222 (1976).

B-8. R.A.J. Shelton, Tran. Faraday Soc. 57, 2113 (1961).

B-9. H.M. Rosenstock, J.R. Sites, J.R. Walton and R. Baldock, J. Chem. Phys. 23, 2442 (1955).

B-10. C.H. Corliss and W.R. Bozman, Nat. Bur. Stand. Monograph, 53, Experimental Transition Probabilities for Spectral Lines of Seventy Elements, U.S. Government Printing Office, Washington, D.C. 1962.

B-11. R.J. Donovan, D. Husain and L.J. Kirsch, Trans. Faraday Soc. 66, 2551 (1970).

B-12. D.W. Trainor (experiments in progress).

B-13. L. Brewer and D.F. Mastick, J. Chem. Phys. 19, 834 (1951).

B-14. K.E. Shuler, J. Chem. Phys. 21, 624 (1953).

APPENDIX C

CROSS SECTIONS FOR THE QUENCHING OF LEAD RESONANCE RADIATION

A. Mandl and Hao-Lin Chen

ABSTRACT

Pb atoms were excited and studied by optical techniques using signal averaging and phase sensitive detection. Cross sections for the quenching of the $^3P_1{}^o$ excited state of Pb were measured by observing the reduction of the atomic fluorescence as a function of foreign gas pressure. The cross sections for the following quenchers measured at 900°K were (in $\AA^2$) N_2, 18; CO, 27; CO_2, 63; CH_4, 55 with an estimated uncertainty of $\pm$ 20%. Upper limits on the quenching cross sections of Ne, Ar, Kr, Xe, H_2, D_2 were also measured.

I. INTRODUCTION

Pulsed gas discharge lasers using metal atoms have been developed over the past decade. Various transitions of Tl, Cu and Pb have been observed to lase.[C-1] Laser action in Pb was first achieved for the resonance-to-metastable level transition corresponding to the 722.9 nm line.[C-2] Other laser transitions observed in Pb have been at 405.8 nm, 364.0 nm and 406.2 nm.[C-3] The kinetics of these systems is, however, not well understood. It is for this reason and for the general purpose of understanding the quenching of metal atom excited states that experimental measurements have been performed to determine the cross sections for quenching of the $6p\ 7s\ ^3P_1^o$ state of lead by Ne, Ar, Kr, Xe, H_2, D_2, CO, CO_2, CH_4 and CF_4. This state is the lowest resonance level of lead and is the origin of the 283.3 nm resonance line. As shown by the energy level diagram in Fig. C-1, it also forms the upper level for the 364.0 nm, 405.8 nm and 722.9 nm lead emission lines. Using a method similar to that of Gibbs,[C-4] the vapor phase lead atoms were produced in a high temperature oven by heating the pure metal. The measurement scheme utilized excitation of the $6s7p\ ^3P_1^o$ state with an AC driven resonance lamp together with phase-sensitive detection.

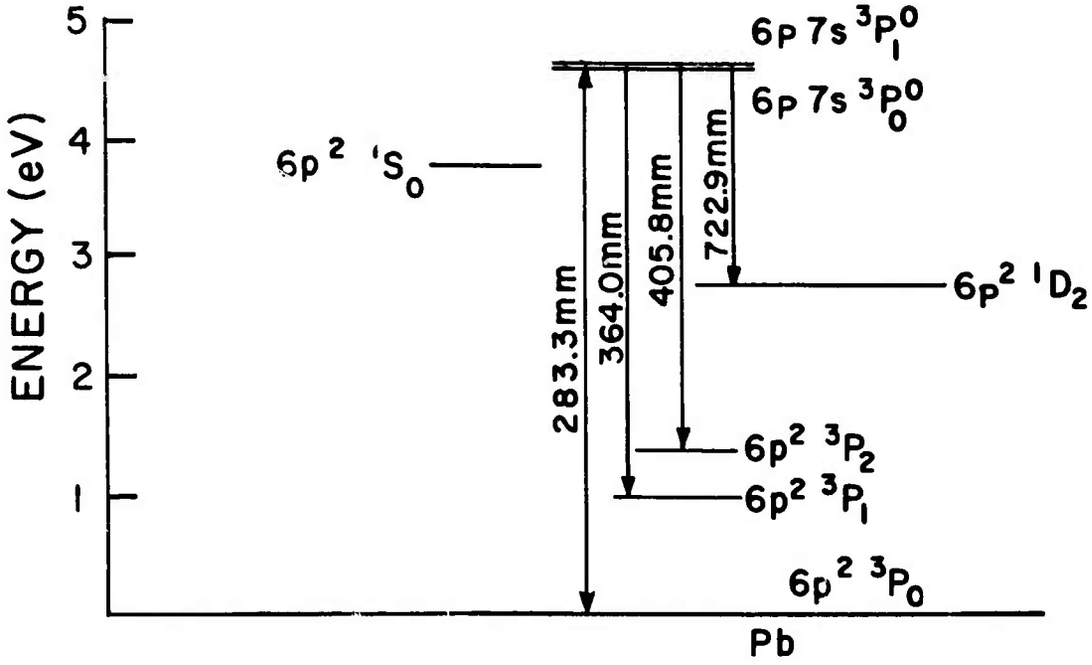

E6994

Fig. C-1 Simplified Energy Level Diagram of Lead

II. EXPERIMENT

A schematic diagram of the apparatus is given in Fig. C-2. The cell is contained in a dual oven system which allows separate control of the lead vapor pressure and lead atom temperature. To ensure that the lead does not condense on the reaction cell walls, the cell is kept ~ 50°K above the side arm temperature containing the lead shot. The oven is made of copper which is heated by alumina insulated nichrome wire. Suprasil quartz windows built into the oven allow passage of the incoming resonance and outgoing fluorescent light. The entire oven is gold plated to inhibit surface oxidation.

The cell is made of suprasil quartz and is an adaptation of a standard spectrophotometer cell with a square cross section of 1 x 1 cm. A magnetically activated quartz valve is attached to the cell to allow introduction of various quenching gases while preventing excessive loss of lead. The cell is pumped to near 10^{-7} Torr with a 2" diffusion pump. Typical lead pressures are 10^{-4} - 10^{-5} Torr and quenching gas pressures varied from one Torr to hundreds of Torr. The diffusion pump, mechanical roughing pump and gas inlet are all coupled to the apparatus through cold traps using liquid N_2 or, for certain cases, a mixture of alcohol and dry ice.

As illustrated, a mercury side arm is also included to introduce Hg into the system for room temperature optical alignment purposes. The Hg was also used for system calibration by performing measurements of the Hg ($^3P_1$) quenching by N_2 as an overall check. This measurement was in good agreement with previous measurements by other experimentors. (C-5, C-6)

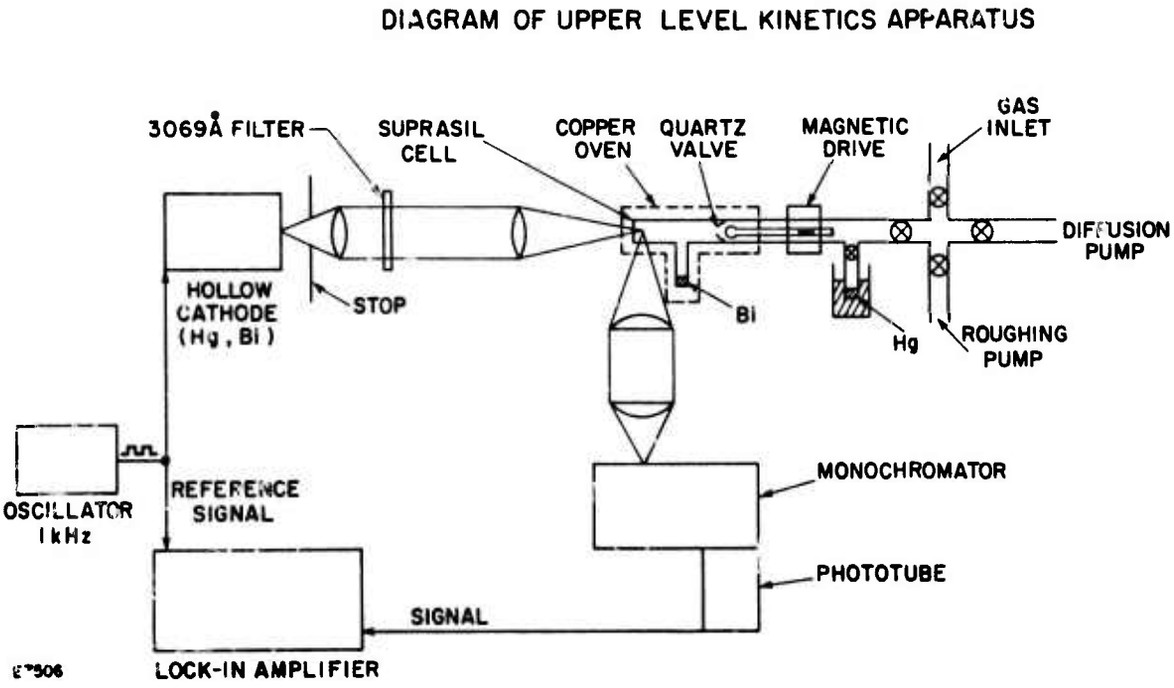

Fig. C-2 Schematic Diagram of Experimental Apparatus

The source of the Pb resonance (283.3 nm) radiation is a Glomax (Barnes Engineering, Inc., Stanford, Conn.) hollow cathode lamp which produces an intense output with good signal to noise. The lamp is electronically chopped using a 1 kc oscillator; this 1 kc signal also serves as a reference for a PAR JB4 lock-in amplifier (Princeton Applied Research, Princeton, N. J.). This convenient experimental procedure avoids the use of a mechanical chopper and in addition, allows the hollow cathode lamp to be pulsed, giving it a greater operating lifetime than when operated continuously. The fluorescence signal is viewed from the side of the cell using a Jarrel Ash 1/4 meter monochrometer and an EMI 9789 QB photo-cathode tube which has a very high gain and extremely low dark current. The signals were read directly from the lock-in amplifier and displayed on an oscilloscope.

Since the Glomax lamp also emits at the detecting wavelength (405.8 nm) its output was passed through a 283.3 nm filter to prevent direct scattering of 405.8 nm radiation to the detection system. This had no effect on the measured quenching cross section but did reduce the overall signal level by about a factor of three.

To be sure that the resonance light was not being trapped in the test cell, measurements were made at a number of lead pressures running over an order of magnitude below the normal operating pressure. If the trapping of resonance radiation were occurring this would affect the lifetime of the Pb ($^3P_1$) state and therefore affect the overall cross section value. Decreasing the Pb pressure reduced the signal level proportionately, but had no effect on the quenching cross sections measured. All of these check-out measurements were made using N_2 as the quenching gas.

III. THEORY OF MEASUREMENT

The lead vapor is excited with incoming radiation $I_{h\nu}$

$$Pb + I_{h\nu} \xrightarrow{k_1} Pb^* \qquad (C-1)$$

where Pb* represents excited Pb ($^3P_1{}^o$).

The excited lead can either be quenched collisionally by a quenching gas M

$$Pb^* + M \xrightarrow{k_2} Pb + M \qquad (C-2)$$

or it can radiate

$$Pb^* \xrightarrow{\tau} Pb + h\nu \qquad (C-3)$$

For completeness we also include self quenching

$$Pb^* + Pb \xrightarrow{k_4} 2Pb \qquad (C-4)$$

The rate equation governing the density of Pb* is

$$\frac{d[Pb^*]}{dt} = k_1 I_{h\nu} [Pb] - k_2 [Pb^*] [M] - [Pb^*]/\tau - k_4 [Pb^*] [Pb] \qquad (C-5)$$

where τ is the lifetime of the Pb ($^3P_1{}^o$) state.

Under steady state conditions, we set $d[Pb^*]/dt = 0$ and solve for $[Pb^*]/\tau$

$$\left(\frac{[Pb^*]}{\tau}\right)_M = \frac{k_1 I_{h\nu} [Pb]}{1 + k_2 [M] \tau + k_4 [Pb] \tau} \qquad (C-6)$$

where the subscript M denotes the presence of a quenching gas M. Since $k_4 \leq 10^{-10}$ cm^3/sec, $\tau = 5.7 \times 10^{-9}$ sec. (C-7) and under the conditions of this experiment Pb $\lesssim 10^{12}$ cm^{-3}, we can neglect the contribution of reaction (C-4) giving,

$$\left(\frac{[Pb^*]}{\tau}\right)_M = \frac{k_1 I_{h\nu}[Pb]}{1 + k_2[M]\tau} \qquad (C\text{-}7)$$

Under conditions where there is no quenching gas present we rewrite (C-7) as

$$\left(\frac{[Pb^*]}{\tau}\right)_0 = k'_1 I_{h\nu}[Pb] \qquad (C\text{-}8)$$

We distinquish in Eqs. (C-7) and (C-8) between k_1 and k_1'. This is because as the pressure in the cell changes, the absorbing line shape changes due to Lorentz broadening. Thus, the overlap between the incident resonance line and the absorbing resonance line changes. If we wish to include the effects of Lorentz and Doppler broadening on the measurement we observe that $k_1 \propto \frac{1}{f(\Delta\nu_D, \Delta\nu_L)}$ where $\Delta\nu_D$ and $\Delta\nu_L$ are the Doppler and Lorentz half widths, respectively. For the case of no quenching gas we would have no Lorentz broadening $k_1' \propto \frac{1}{\Delta\nu_D}$.

We can now take the ratio of Eq. (C-7) and (C-8) and define this as

$$R = \frac{([Pb^*]/\tau)_0}{([Pb^*]/\tau)_M} = (1 + k_2[M]\tau)\ \frac{f(\Delta\nu_D, \Delta\nu_L)}{\Delta\nu_D} \qquad (C\text{-}9)$$

For low pressures $\Delta\nu_L \ll \Delta\nu_D$, so $f(\Delta\nu_D, \Delta\nu_L) \to \propto \Delta\nu_D$, and

$$R \to 1 + k_2[M]\tau \qquad (C\text{-}10)$$

This is just the usual Stern-Volmer[C-8] expression. Thus a plot of the ratio of the nonquenched to the quenched fluorescent signals from lead as a function of quenching gas pressure, gives a straight line with intercept 1 and slope $k_2\tau$. Since τ is known for the $^3P_1{}^o$ state of lead, k_2, the rate of quenching can be derived.

For high pressures

$$\Delta\nu_L \gg \Delta\nu_D$$

so

$$f(\Delta\nu_D, \Delta\nu_L) \rightarrow \propto \Delta\nu_L$$

and

$$\Delta\nu_L \propto [M]$$

So

$$R \sim ([M] + k_2[M]^2) \frac{1}{\Delta\nu_D} \qquad \text{(C-11)}$$

Thus at high pressure a plot of R vs [M] should become parabolic. This is shown schematically in Fig. (C-3).

By using this measurement technique and plotting the data as in Fig. (C-3), one can learn about the broadening in a resonance lamp. Thus, instead of using a very high resolution monochromator to analyze the resonance line from a lamp, one could plot a modified Stern-Volmer curve (Fig. C-3) and observe where the curve goes from a straight line to a parabola, and crudely estimate the amount of broadening in the lamp.

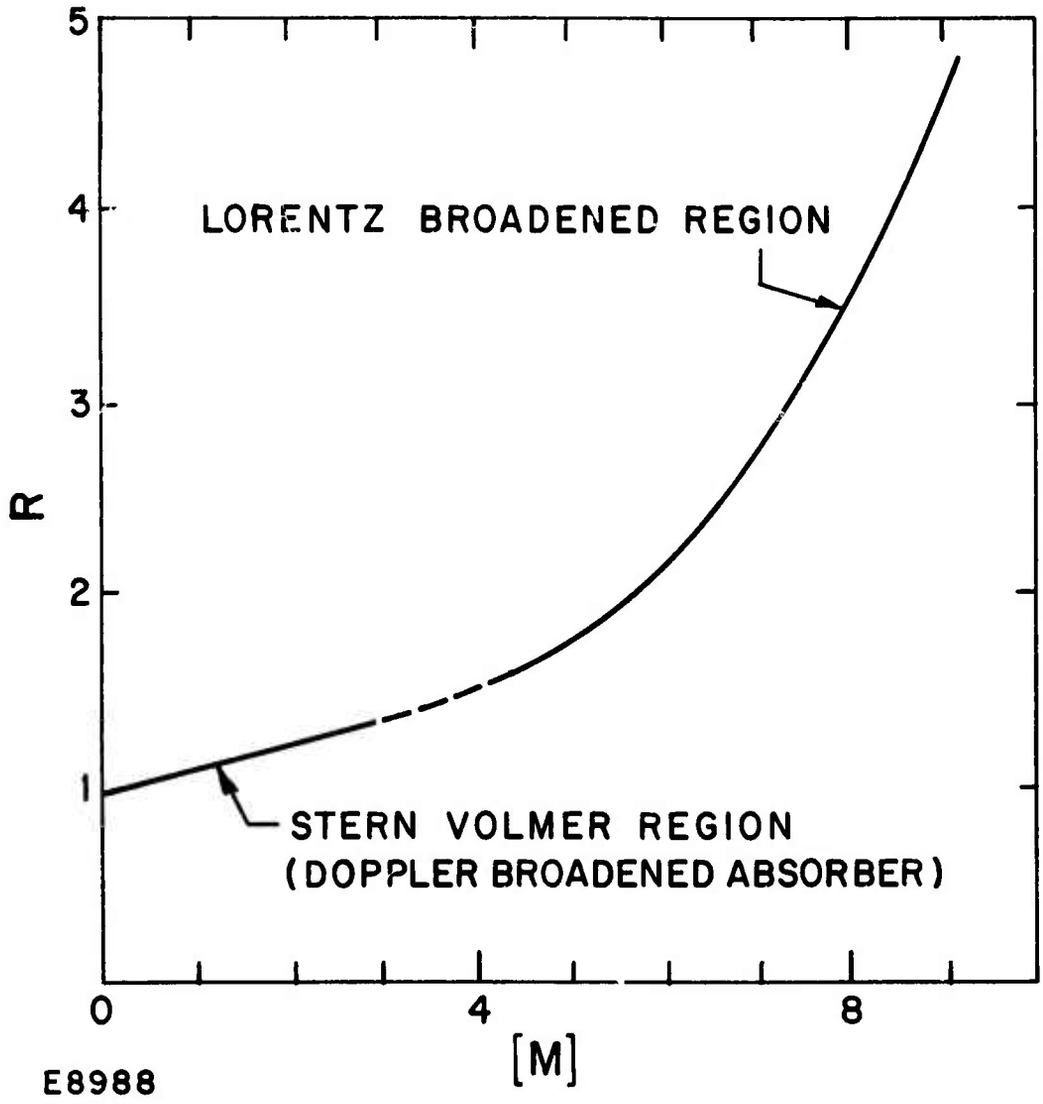

Fig. C-3 Generalized Curve of R vs [M] (arbitrary units) Illustrating the High Pressure Parabolic Dependence Expected Due to Lorentz Broadening

IV. MEASUREMENTS

The system was initially aligned and tested by performing a mercury resonance fluorescence experiment. A mercury hollow cathode lamp was used and resonance 253.7 nm scattering was observed. Once this signal was peaked the mercury was pumped out of the system, and the ovens were turned on. The cell was always kept at a temperature of ~ 50°K above the lead reservoir. The lead was substituted for the mercury hollow cathode and the 283.3 nm resonance radiation was focused into the cell. All of the lead lines (i.e., 283.3, 364.0 or 405.8 nm) were observed but most of the measurements were made at 405.8 nm.

By not utilizing the 283.3 nm fluorescence line one avoids possible problems of complications in the data analysis arising from scattering of this resonance line. It is important to note, however, that pressures must be low enough to prevent the 283.3 nm radiation from trapping, since this would affect the lifetime of the Pb ($^3P_1$) state and therefore affect the cross sections. As mentioned in Section II this effect was checked by varying the [Pb] over an order of magnitude as follows: Normal operation had [Pb] = 3.3×10^{12} cm^{-3} (T = 840°K) and by analog to the work of Michael & Yeh[C-9] one would expect little imprisonment of the 283.3 nm radiation at this concentration. As a check, however, [Pb] was reduced to [Pb] = 5.5×10^{11} cm^{-3} (T = 780°K) and no significant affect on the quenching rates of Pb by N_2 was observed; these experimental results are presented in Fig. (C-4).

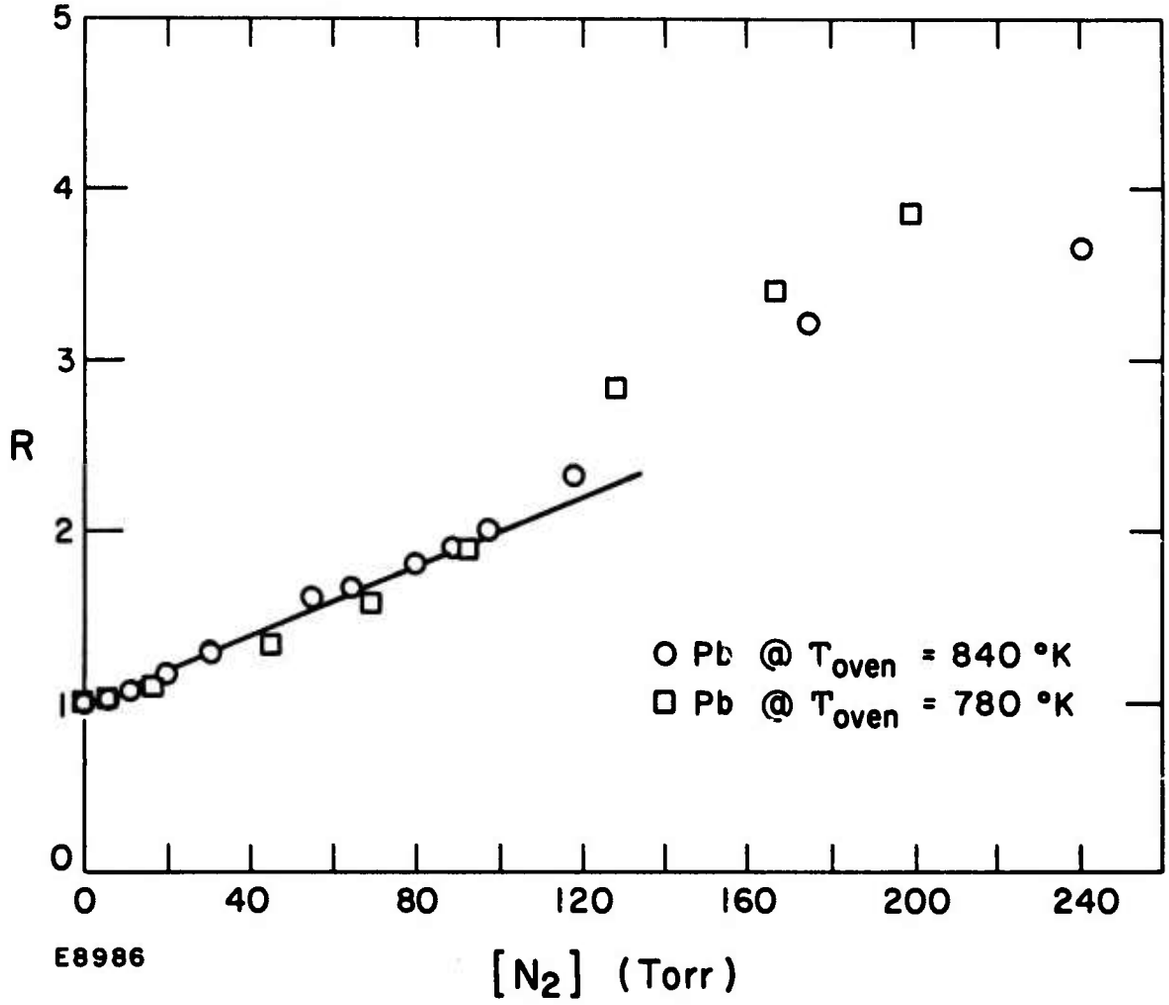

Fig. C-4 Stern-Volmer Plot for the Quenching of Pb* by N_2. The Pb concentration was varied by changing the oven temperature. Since the data shows no dependence of the Pb concentration, this implies no concentration this implies no significant self-trapping of the resonance line.

The various quenching cross sections measured are listed in Table C-1. Also listed in Table C-1 are cross section measurements of Gibbs[C-4] and Jenkins[C-10] for comparison.

TABLE C-1

MEASURED LEAD QUENCHING CROSS SECTIONS

$Pb\ (^3P_1^o) + Q \rightarrow Pb + Q$

Q	Jenkins $(\pi\sigma^2)$ $\mathring{A}^2$	Gibbs $\mathring{A}^2$	Present Exp. $\pm$ 20% $\mathring{A}^2$
Ne		< .1	< .05
Ar	≈ 0 < 5	< .1	< .3
Kr			<1.3
Xe		< .4	< .8
H_2	1.3 ± .3	< .3	< .05
D_2		< .9	< .08
N_2	17.9 ± 1.6	16 ± 8	18
CO	40.8 ± 9.4		27
CO_2	91.1 ± 15.7		63
CH_4			55
CF_4			~ 200
SF_6			> 200

V. DISCUSSION

The measurements fall into three categories based on the magnitude of the measured cross section. For the first group, the measurements resulted in linear Stern-Volmer plots. For these cases, useful fluorescence radiation decay rates are observed in the range of tens of Torr up to a couple of hundred Torr and the interpretation of the cross section from the slope of a Stern-Volmer plot is quite straightforward. This group includes N_2, CO, CO_2, CH_4. These species all have cross sections which are tens of $\AA^2$.

Members of the second group have a much smaller cross section for quenching, typically < 1 $\AA^2$. Only an upper bound to the cross section can be inferred. For these gases, Ne, Ar, Kr, Xe, H_2 & D_2 no measurable decrease in the fluorescence signal was observed with quenching gases at pressures up to ~ 200 Torr. At higher pressures broadening effects complicated data analysis as discussed in Section III. The cross sections listed are therefore upper bounds obtained by including systematic uncertainties and the measured signal-to-noise. A typical curve from this group is shown in Fig. (C-5), where the decrease in the fluorescence signal for the Pb ($^3P_1$) state as measured at 405.8 nm is plotted as a function of Xe pressure. One can see that at high pressure the points, R, follow a somewhat parabolic curve as predicted in Eq. C-11. It is possible from a curve like this to estimate width of the Pb resonance source. We estimate that under the conditions of this experiment the lamp 283.3 nm line was roughly broadened to 0.77 cm^{-1}.

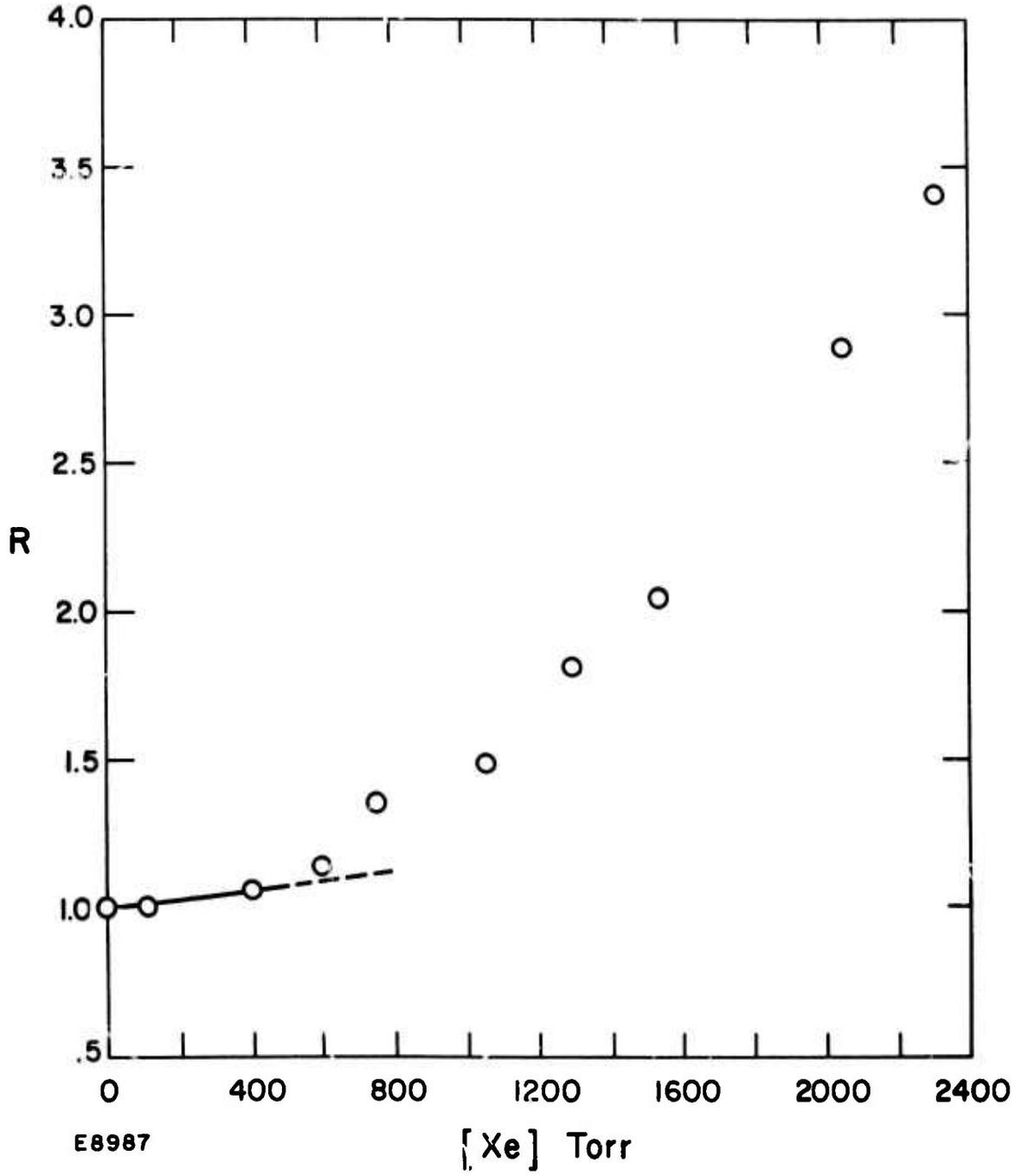

Fig. C-5 Stern-Volmer Plot for the Quenching of Pb* by Xenon Gas. Above 400 Torr one sees the non-linearity in the curve due to broadening effects as discussed in Section III.

Gases in the third group (CF_4, SF_6) have extremely large cross sections. Although we have no direct evidence, one possible explanation of these fast rates could be a chemical reaction channel available for these cases. Thus, in addition to the quenching reaction

$$Pb^* + CF_4^- \rightarrow Pb + CF_4 \qquad \text{(C-12)}$$

one could have chemical reaction, e.g.,

$$Pb^* + CF_4 \rightarrow PbF + CF_3 \qquad \text{(C-13)}$$

which is exothermic by about 50 kcal/mole. The "Stern-Volmer" plot for CF_4 quenching is shown in Fig. (C-6). In this case, a few Torr of CF_4 shows "quenching" of Pb*; the implied cross section is significantly larger than in the previous two groups. The apparent parabolic dependence in this case cannot be due to Lorentz broadening as manifest in the second case, but might possibly be due to some chemical effects. If for example a chemical reaction between the lead and the quenching gas were producing a species which is absorbing at the incident wavelength (283.3 nm) then the incident light in the cell is reduced as

$$I_{cell} = I_{h\nu}\, e^{-[A]\, l\alpha} \qquad \text{(C-14)}$$

where A is the chemically produced species which absorbs at 283.3 nm, l is the path length in the cell and α is the cross section for absorption. If one now substitutes this term into Eq. (C-9) in the limit of low pressures one finds

$$R = (1 + k_2 [M]\, \tau)\, e^{[A]\, l\alpha} \qquad \text{(C-15)}$$

[A] is proportional to the density of quenching gas [M]. If one now expands the exponential in (C-13) one again finds that there is an M^2 dependence for R.

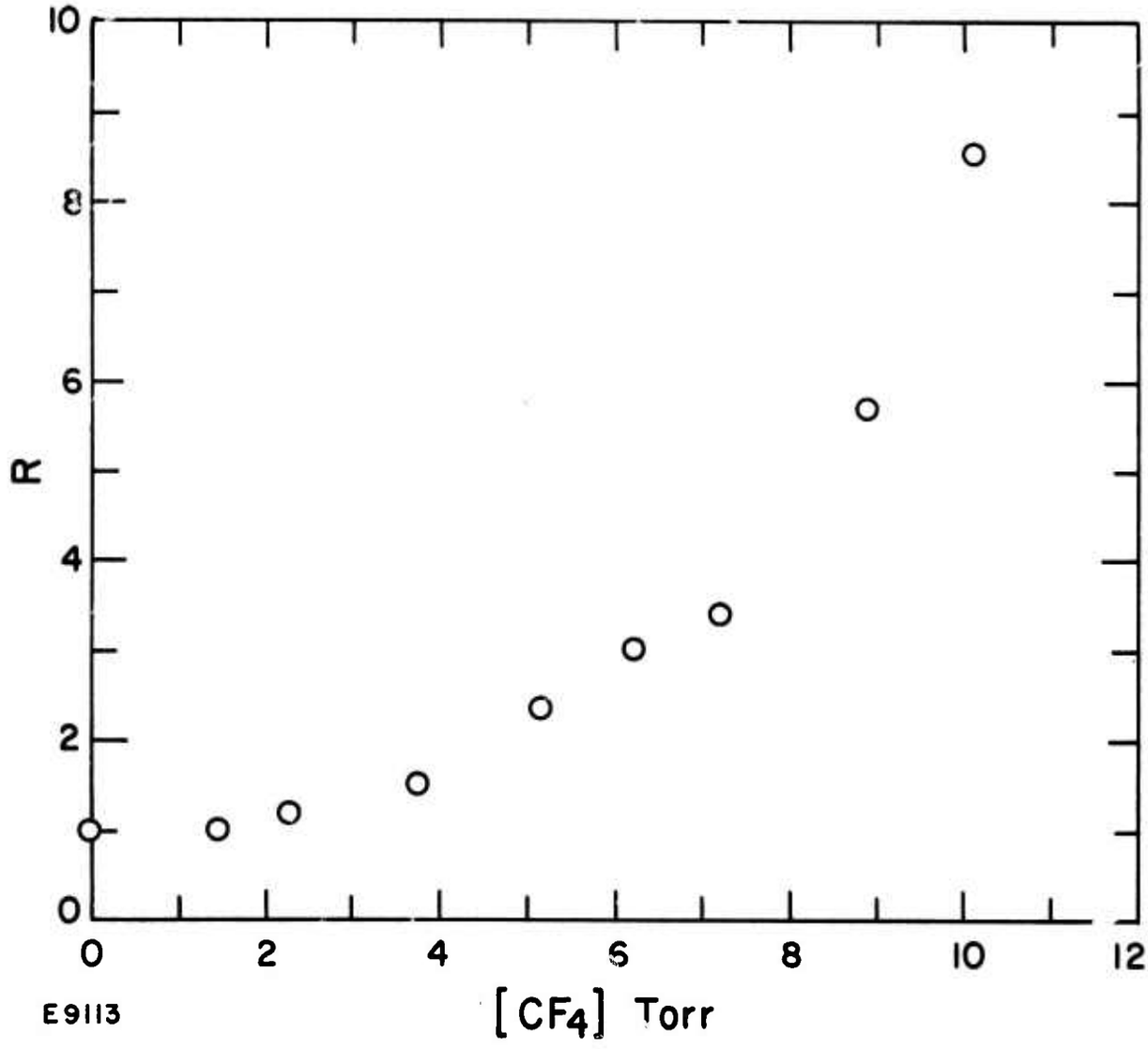

Fig. C-6 Stern-Volmer Plot for the Quenching of Pb* by CF_4. The curvature is discussed in the text.

Thus, a chemical explanation of the data is possible, although we have not identified an absorbing species in this case.

It should be noted that Jenkins[C-7] quotes all his cross sections as σ^2 (collision diameter squared), so all his values have been multiplied by π for comparison (in Table C-I) with this work and with Gibbs. The error limits which should be assigned to this work when taking into account noise fluctuations in the signal level and uncertainties in the lifetime of the upper state are about $\pm$ 20%. Thus, the comparison between this work and both Gibbs and Jenkins looks quite good for most cases.

Our H_2 results are in agreement with Gibbs but substantially lower than Jenkins. These measurements were repeated several times. In this case any impurity in our system would have tended to increase the cross section. Since we measured the lowest value, we feel that it is probably correct.

ACKNOWLEDGMENTS

The authors wish to thank Drs. S. Mani and J. J. Ewing for some very helpful discussions. We also wish to thank W. Fyfe for his technical assistance in setting up the experiment and accumulating the data. This was a most important contribution to this program.

APPENDIX C

REFERENCES

C-1. Petrash, G. G., Soviet Physics Vspekki 14, 747 (1972). This is a good review of pulsed gas discharge lasers through 1970.

C-2. Fowles, G. R. and Silfvest, W. T., Appl. Phys. Lett. 6, 236 (1965).

C-3. Isaev, A. A. and Petrash G. G., ZhETF Pis. Red. 10, 188 (1969), JETP Lett. 10, 119 (1969).

C-4. Gibbs, H. M., Phys. Rev. A 5, 2408 (1972).

C-5. Calvert, J. G. and Pitts, Jr., J. N., Photochemistry (Wiley, New York 1966).

C-6. Zemansky, M. W., Phys. Rev. 36, 919 (1930).

C-7. Saloman, E. B. and Happer, W., Phys. Rev. 144, 7 (1966).

C-8. Stern, O. and Volmer, M., Z. Physik 20, 183 (1919).

C-9. Michael, J. V. and Yeh, C., J. Chem. Phys. 53, 59 (1970).

C-10. Jenkins, D. R., Proc. Roy. Soc. London A 313, 551 (1969).

DISTRIBUTION LIST FOR CONTRACT NO: N00014-75-C-0061

Office of Naval Research, Department of the Navy, 800 North Quincy Street, Arlington, VA 22217, Attn: Physics Program (421) (3 copies)

Naval Research Laboratory, Department of the Navy, Washington, D.C. 20375, Attn: Technical Library, (1 copy)

Office of the Director of Defense, Research and Engineering, Information Office Library Branch, The Pentagon, Washington, D.C. 20301 (1 copy)

U.S. Army Research Office, Box CM Duke Station, Durham, NC 27706 (1 copy)

Defense Documentation Center, Cameron Station, Alexandria, VA 22314 (12 copies)

Defender Information Analysis Center, Battelle Memorial Institute, 505 King Avenue, Columbus, OH 43201 (1 copy)

Director, Office of Naval Research Branch Office, 536 South Clark Street, Chicago, IL 60615 (1 copy)

San Francisco Area Office, Office of Naval Research, 760 Market Street, Room 447, San Francisco, CA 94102 (1 copy)

Air Force Office of Scientific Research, Department of the Air Force, Washington, D.C. 22209 (1 copy)

Office of Naval Research Branch Office, 1030 East Green Street, Pasadena, CA 91106 (1 copy)

Code 102 IP (ONRL), Office of Naval Research, 800 North Quincy Street, Arlington, VA 22217 (6 copies)

Defense Advanced Research Projects Agency, 1400 Wilson Blvd., Arlington VA 22209, Attn: Director, Laser Division (1 copy)

ODDR&E, Pentagon, Washington, D.C. 20301, Attn: Assistant Director (Space and Advanced Systems) (1 copy)

Office of the Assistant Secretary of Defense, System Analysis (Strategic Programs) Washington, D.C. 20301, Attn: Mr. Gerald R. McNichols (1 copy)

U.S. Arms Control and Disarmament Agency, Department of State Building, Room 4931, Washington, D.C. 20451, Attn: Dr. Charles Henkin (1 copy)

Energy Research Development Agency, Division of Military Applications, Washington, D.C. 20545 (1 copy)

National Aeronautics and Space Administration, Lewis Research Center, Cleveland, OH 44135, Attn: Dr. John W. Dunning, Jr. (1 copy)
(Aerospace Res. Engineer)

National Aeronautics & Space Administration, Code RR, FOB 10B, 600 Independence Avenue, SW, Washington, D.C. 20546 (1 copy)

National Aeronautics and Space Administration, Ames Research Center, Moffet Field, CA 94035, Attn: Mr. Robert L. McKenzie (1 copy)
Dr. Kenneth W. Billman (1 copy)

Department of the Army, Office of the Chief of RD&A, Washington, D.C. 20310, Attn: DARD-DD (1 copy)
DAMA-WSM-T (1 copy)

Department of the Army, Office of the Deputy Chief of Staff for Operations & Plans, Washington, D.C. 20310, Attn: DAMO-RQD (2 copies)

Ballistic Missile Defense Program Office (BMDPO), The Commonwealth Bldg., 1300 Wilson Blvd., Arlington, VA 22209, Attn: Mr. Albert J. Bast, Jr.
(3 copies)

U.S. Army Missile Command, Research and Development Division, Redstone Arsenal, ALA 35809, Attn: Army High Laser Energy Programs (2 copies)

Commander, Rock Island Arsenal, Rock Island, IL 61201, Attn: SARRI-LR, Mr. J.W. McCarvey (1 copy)

Commanding Officer, U.S. Army Mobility Equipment R&D Center, Ft. Belvior, VA 22060, Attn: SMEFB-MW (1 copy)

Commander, U.S. Army Armament Command, Rock Island, IL 61201, Attn: AMSAR-RDT (1 copy)

Director, Ballistic Missile Defense Advanced Technology Center, P.O. Box 1500, Huntsville, AL 35807, Attn: ATC-O (1 copy)
ACT-T (1 copy)

Commander, U.S. Army Material Command, Alexandria, VA 22304, Attn: Mr. Paul Chernoff (AMCRD-T) (1 copy)
Dr. B. Zarwyn (AMCRD-T) (1 copy)

Commanding General, U.S. Army Munitions Command, Dover, NH 07801, Attn: Mr. Gilbert F. Chesnov (AMSMU-R) (1 copy)

Director, U.S. Army Ballistic Res. Lab., Aberdeen Proving Ground, MD 21005, Attn: Dr. Robert Eichelberger (1 copy)
Mr. Frank Allen (1 copy)
Dr. E.C. Alcarez (1 copy)

Commandant, U.S. Army, Air Defense School, Ft. Bliss, TX 79916, Attn: Air Defense Agency (1 copy)
ATSA-CTD-MS (1 copy)

Commanding General, U.S. Army Combat Dev. Command, Ft. Belvior, VA 22060, Attn: Director of Material, Missile Div. (1 copy)

Commander, U.S. Army Training & Doctrine Command, Ft. Monroe, VA 23651, Attn: ATCD-CF (1 copy)

Commander, U.S. Army Frankford Arsenal, Philadelphia, PA 19137, Attn: Mr. M. Elnick SARFA-FCD, Bldg. 201-3 (1 copy)

Commander, U.S. Army Electronics Command, Ft. Monmouth, NJ 07703, Attn: AMSEL-CT-L, Dr. R.C. Buaer (1 copy)

Commander, U.S. Army Combined Arms Combat Developmenta Activity, Ft. Leavenworth, KS 66027 (1 copy)

National Security Agency, Ft. Geo. C. Meade, MD 20755, Attn: R.C. Foaa A763 (1 copy)

Deputy Commandant for Combat & Training Developmenta, U.S. Army Ordnance Center and School, Aberdeen Proving Ground, MD 21005
Attn: ATSL-CTD-MS-R (1 copy)

Commanding Officer, USACDC CBR Agency, Ft. McClellan, AL 36201, Attn: CDCCBR-MR (Mr. F.D. Poer) (1 copy)

DISTRIBUTION LIST FOR CONTRACT NO: N00014-75-C-0061 (Continued)

Department of the Navy, Office of the Chief of Naval Operations, Pentagon 5C739, Washington, D.C. 20350, Attn: (OP982F3) (1 copy)

Office of Naval Research, 495 Summer Street, Boston, MA 02210, Attn: Dr. A. D. Wood (1 copy)

Department of the Navy, Deputy Chief of Naval Material (Dev.) Washington, D.C. 20360, Attn: Mr. R. Gaylord (MAT 032B) (1 copy)

Naval Missile Center, Point Mugu, CA 93042, Attn: Gary Gibbs (Code 5352) (1 copy)

Naval Research Lab., Washington, D.C. 20375, Attn: (Code 5503-LTPO) (1 copy)
Dr. P. Livingston (Code 55060) (1 copy)
Dr. A.1 Schindler (Code 6330) (1 copy)
Dr. H. Shenker (Code 6530) (1 copy)
Mr. D.J. McLaughlin (Code 5560) (1 copy)
Dr. John L. Walsh (Code 5503) (1 copy)

High Energy Laser Project Office, Department of the Navy, Naval Sea Systems Command, Washington, D.C. 20360, Attn: Capt. J.G. Wilson, USN (PMS-405) (1 copy)

Superintendent, Naval Postgraduate School, Monterey, CA 93940, Attn: Library (Code 2124) (1 copy)

Navy Radiation Technology Liaison Office, Air Force Weapons Lab. (NLO), Kirtland AFB, NM 87117, (1 copy)

Naval Surface Weapons Center, White Oak, Silver Spring, MD 20910, Attn: Dr. Leon H. Schindel (Code 310) (1 copy)
Dr. E. Leroy Harris (Code 313) (1 copy)
Mr. K. Enkenhus (Code 034) (1 copy)
Mr. J Wise (Code 047) (1 copy)
Technical Library (1 copy)

U.S. Naval Weapons Center, China Lake, CA 93555, Attn: (Code 5114) (1 copy)
Technical Library (1 copy)

HQ USAF (AF/RDPS), Pentagon, Washington, D.C. 20330, Attn: Lt. Col. A J. Chiota (1 copy)

HQ AFSC/XRLW, Andrews AFB, Washington, D.C. 20331, Attn: Maj. J M. Walton, (1 copy)

HQ AFSC (DLCAW), Andrews AFB, Washington, D.C. 20331, Attn: Maj. H. Axelrod (1 copy)

Air Force Weapons Lab., Kirtland AFB, NM 87117, Attn: LR (4 copies)
AL (2 copies)

HQ SAMSO (XRTD), P.O. Box 92960, Worldway Postal Center, Los Angeles, CA 90009, Attn: Lt. Dorian DeMaio (XRTD) (1 copy)

AF Avionics Lab (TEO), Wright Patterson AFB, OH 45433, Attn: Mr. K. Hutchinson (1 copy)

Dept. of the Air Force, Air Force Materials Lab. (AFSC), Wright Patterson AFB, OH 45433, Attn: Maj. Paul Elder (LPS) (1 copy)
Laser Window Group

HQ Aeronautical Systems Div., Wright Patterson AFB, OH 45433, Attn: XRF - Mr. Clifford Fawcett (1 copy)

Rome Air Development Command, Griffiss AFB, Rome NY 13440, Attn: Mr. R. Urtz (OCSE) (1 copy)

HQ Electronics Systems Div. (ESL), L.G. Hanscom Field, Bedford, MA 01730, Attn: Mr. Alfred E. Anderson (XRT) (1 copy)
Capt. James C. Jalbert (XRJ) (1 copy)
Technical Library (1 copy)

Air Force Rocket Propulsion Lab., Edwards AFB, CA 93523, Attn: B.R. Bornhorst, (LKCG) (1 copy)

Air Force Aero Propulsion Lab., Wright Patterson AFB, OH 45433, Attn: Col. Walter Moe (CC) (1 copy)

Dept. of the Air Force, Foreign Technology Division, Wright Patterson AFB, OH 45433, Attn: PDTN (1 copy)

CINCSAC/INEP, Offutt AFB, NE 68113 (1 copy)

Commandant of the Marine Corps, Scientific Advisor (Code RD-1), Washington, D.C. 20380, (1 copy)

USAF/INAKA, Washington, D.C. 20330, Attn: Lt. Col. W.M. Truesdell. (1 copy)

Aerospace Research Labs., (LP), Wright Patterson AFB, OH 45433, Attn: Lt. Col. Max Duggina (1 copy)

Defense Intelligence Agency, Washington, D.C. 20301, Attn: Mr. Seymour Berler (DT1B) (1 copy)

Central Intelligence Agency, Washington, D.C. 20505, Attn: Mr. Julian C. Nall, (1 copy)

Analytic Services, Inc., 5613 Leesburg Pike, Falls Church, VA 22041, Attn: Dr. John Davis (1 copy)

Aerospace Corp., P.O. Box 92957, Los Angeles, CA 90009, Attn: Dr. G.P. Millburn (1 copy)

Airesearch Manuf. Co., 9851 - 9951 Sepulveda Blvd., Los Angeles, CA 90009, Attn: Mr. A. Colin Stancliffe (1 copy)

Atlantic Res. Corp., Shirley Highway at Edsall Road, Alexandria, VA 22314, Attn: Mr. Robert Naismith (1 copy)

AVCO Everett Research Lab., 2385 Revere Beach Parkway, Everett, MA 02149, Attn: Dr. George Sutton (1 copy)
Dr. Jack Daugherty (1 copy)

Battelle Columbus Laboratories, 505 King Avenue, Columbus, OH 43201, Attn: Mr. Fred Tietzel (STOLAC) (1 copy)

Bell Aerospace Co., Buffalo, NY 14240, Attn: Dr. Wayne C. Solomon, (1 copy)

Boeing Co., P.O. Box 3999, Seattle, WA 98124, Attn: Mr. M.1. Gemble (2-1460, MS 8C-88) (2 copies)

Electro-Optical Systems, 300 N. Halstead, Pasadena, CA 91107, Attn: Dr. Andrew Jensen (1 copy)

ESL Inc., 495 Java Drive, Sunnyvale, CA 94086, Attn: Arthur Einhorn (1 copy)

DISTRIBUTION LIST FOR CONTRACT NO: N00014-75-C-0061 (Continued)

General Electric Co., Space Division, P.O. Box 8555, Philadelphia, PA 19101, Attn: Dr. R.R. Sigismonti (1 copy)
Dr. C.E. Anderson (1 copy)

General Electric Co., 100 Plastics Avenue, Pittsfield, MA 01201, Attn: Mr. D.G. Harrington (Room 1044) (1 copy)

General Research Corp., P.O. Box 3587, Santa Barbara, CA 93105, Attn: Dr. R. Holbrook (1 copy)

General Research Corp., 1501 Wilson Blvd., Suite 700, Arlington, VA 22209, Attn: Dr. Giles F. Crimi (1 copy)

Hercules, Inc., Industrial System Dept., Wilmington, DE 19899, Attn: Dr. R.S. Voris (1 copy)

Hercules, Inc., P.O. Box 210, Cumberland, MD 21502, Attn: Dr. Ralph R. Preckel (1 copy)

Hughes Research Labs., 3011 Malibu Canyon Road, Malibu, CA 09265, Attn: Dr. D. Forster (1 copy)
Dr. A.N. Chester (1 copy)
Dr. Viktor Evtuhov (1 copy)

Hughes Aircraft Co., Aerospace Group - Systems Division, Canoga Park, CA 91304, Attn: Dr. Jack A. Alcalay (1 copy)

Hughes Aircraft Co., Centinela and Teale Streets, Bldg. 6, MS e-125, Culver City, CA 90230, Attn: Dr. William Yates (1 copy)

Institute for Defense Analysis, 400 Army Navy Drive, Arlington, VA 22202, Attn: Dr. Alvin Schnitzler (1 copy)

John Hopkins University, Applied Physics Lab., 8621 Ga. Avenue, Silver Spring, MD 20910, Attn: Dr. Albert M. Stone (1 copy)
Dr. R.E. Gorozdos (1 copy)

Lawrence Livermore Lab., P.O. Box 808, Livermore, CA 94550, Attn: Dr. R.E. Kidder (1 copy)
Dr. E. Teller (1 copy)
Dr. Joe Fleck (1 copy)

Los Alamos Scientific Lab., P.O. Box 1663, Los Alamos, NM 87544, Attn: Dr. Keith Boyer (1 copy)

Lulejian and Associates, Inc., Del Amo Financial Center, Suite 500, 21515 Hawthorne Blvd., Torrance, CA 90503 (1 copy)

Lockheed Palo Alto Res. Lab., 3251 Hanover Street, Palo Alto, CA 94303, Attn: L.R. Lunsford, Orgn. 52-24 Bldg. 201 (1 copy)

Mathematical Sciences Northwest, Inc., P.O. Box 1887, Bellevue, WN 98009, Attn: Mr. Peter H. Rose (1 copy)
Dr. Abraham Hertzberg (1 copy)

Martin Marietta Corp., P.O. Box 179, Mail Station 0471, Denver, CO 80201, Attn: Mr. Stewart Chapin (1 copy)
Mr. Scott Giles (1 copy)

Massachusetts Institute of Technology LINCOLN LAB., P.O. Box 73, Lexington, MA 02173 Attn: Dr. S. Edelberg (1 copy)
Dr. L.C. Marquet (1 copy)
Dr. J. Freedman (1 copy)
Dr. G.P. Dinneen (1 copy)
Dr. R.H. Rediker (1 copy)

McDonnel Douglas Astronautics Co., 5301 Bolsa Avenue, Huntington Beach, CA 92647, Attn: Mr. P.L. Klevatt (1 copy)
Dept. A3-830-BBFO, M/S 9 (1 copy)

McDonnel Douglas Res. Labs., Dept. 220, Box 516, St. Louis, MO 56166, Attn: Dr. D.P. Ames (1 copy)

MITRE Corp., P.O. Box 208, Bedford, MA 01730, Attn: Mr. A.C. Cron (1 copy)

North American Rockwell Crop., Autonetics Div., 3370 Miraloma Avenue, Anaheim, CA 92803, Attn: Mr. T.T. Kumagi (1 copy)
C/476 Mail Code HA18

Northrop Corp., 3401 West Broadway, Hawthorne, CA 90250, Attn: Dr. Gerard Hasserjian, Laser Systems Dept. (1 copy)

Dr. Anthony N. Pirri, Physical Sciences Inc., 18 Lakeside Office Park, Wakefield, MA 01880 (1 copy)

RAND Corp, 1700 Main Street, Santa Monica, CA 90406, Attn: Dr. Claude R. Culp/Mr. G.A. Carter (1 copy)

Raytheon Co., 28 Seyon Street, Waltham, MA 02154, Attn: Dr. Frank A. Horrigan (Res. Div.) (1 copy)

Raytheon Co. (Equipment Division), Boston Post Road, Sudbury, MA 01776, Attn: Dr. Charles Sonnenschien (1 copy)

Raytheon Co., Bedford Labs., Missile Systems Div., Bedford, MA 01730, Attn: Dr. H.A. Mehlhorn (1 copy)

Riverside Research Institute, 80 West End Street, New York, NY 10023, Attn: Dr. L.H. O'Neill (1 copy)
Dr. John Bose (1 copy)
Miss Helen Cressman (HPEGL Library) (1 copy)

R&D Associates, Inc., P.O. Box 3580, Santa Monica, CA 90431, Attn: Dr. R.E. LeLevier (1 copy)
Dr. R. Hundley (1 copy)

Rockwell International Corp., 3370 Miraloma Corp., Anaheim, CA 92803, Attn: R.E. Hovda (DB 29) (1 copy)
Dr. J. Winocur (D/528, HA14) (1 copy)

Rockwell International Corp. Ricketdyne Div., Albuquerque District Office, 3636 Menaul Blvd, NE, Suite 211, Albuquerque, NM 87110
Attn: C.K. Kraus, Mgr. (1 copy)

SANDIA Corp., P.O. Box 5800, Albuquerque, NM 87115, Attn: Dr. Al Narath (1 copy)

Stanford Research Institute, Menlo Park, CA 94025, Attn: Dr. H.E. Lindberg (1 copy)
Dr. J.E. Mahek (1 copy)

Science Applications Inc., 1911 N. Ft. Meyer Drive, Arlington, VA 22209, Attn: L. Peckham (1 copy)

Science Applications Inc., P.O. Box 328, Ann Arbor, MI 48103, Attn: R.E. Meredith (1 copy)

Science Applications Inc., 6 Preston Court, Bedford, MA 01730, Attn: R. Greenberg (1 copy)

Science Applications Inc., P.O. Box 2351, La Jolla, CA 92037, Attn: Dr. John Asmus (1 copy)

Systems, Science and Software, P.O. Box 1620, La Jolla, CA 92037, Attn: Alan F. Klein (1 copy)

Systems Consultants, Inc., 1050 31st Street NW, Washington, D.C. 20007, Attn: Dr. R.B. Keller (1 copy)

Thiokol Chemical Corp., WASATCH Div., P.O. Box 524, Brigham City, UT 84302, Attn: Mr. J.E. Hansen (1 copy)

TRW Systems Group, One Space Park, Bldg. R-1 RM 1050, Redondo Beach, CA 90278, Attn: Mr. Norman Campbell (1 copy)

DISTRIBUTION LIST FOR CONTRACT NO: N00014-75-C-0061 (Continued)

United Aircraft Res. Labs., 400 Main Street, East Hartford, CT 06108, Attn: Mr. G. H. McLafferty (3 copies)
Mr. Albert Angelbeck (1 copy)

United Aircraft Corp., Pratt and Whitney Acft. Div., Florida R&D Center, West Palm Beach, FL 33402, Attn: Dr. R. A. Schmidtke (1 copy)
Mr. Ed Pinsley (2 copies)

VARIAN Associates, EIMAC Div., 301 Industrial Way, San Carlos, CA 94070, Attn: Mr. Jack Quinn (1 copy)

Vought Systems Div., LTV Aerospace Corp., P. O. Box 5907, Dallas, Tx 75222, Attn: Mr. F. G. Simpson, Mail Station 254142 (1 copy)

Westinghouse Electric Corp., Defense and Space Center Friendship International Airport - Box 746, Baltimore, MD 21203
Attn: Mr. W. F. List (3 copies)

Westinghouse Res. Labs., Beulah Road, Churchill Boro, Pittsburgh, PA 15235, Attn: Dr. E. P. Riedel (1 copy)
Mr. R. L. Hundstad (1 copy)

United Aircraft Company Research Laboratories, East Hartford, Ct 06108, Attn: A. J. DaMaria (1 copy)

Airborne Instruments Laboratory, Walt Whitorian Road, Melville, NY 11746, Attn: F. Pace (1 copy)

Stanford Research Institute, Menlo Park, CA 94025, Attn: Dr. F. T. Smith (1 copy)

General Electric R&D Center, Schenectady, NY 12305, Attn: Dr. Donald White (1 copy)

Cleveland State University, Cleveland, OH 44115, Attn: Dean Jack Soules (1 copy)

Esso Research and Engineering Co., P. O. Box 8, Linden, NH 07036, Attn: D. Crafstein (1 copy)

University of Maryland, Department of Physics and Astronomy, College Park, MD 20742, Attn: D. Curry (1 copy)

Sylvania Electric Products, Inc., 100 Fergeson Drive, Mountain View, CA 94040, Attn: L. M. Osterink (1 copy)

North American Rockwell Corp., Autonetics Division, 3370 Miraloma Avenue, Anaheim, CA 92803, Attn: R. Gudmundsen (1 copy)

Massachusetts Institute of Technology, 77 Massachusetts Avenua, Cambridge, MA 02138, Attn: Prof. A. Javan (1 copy)

Lockheed Missile & Space Co., Palo Alto Research Laboratories, Palo Alto, CA 94304, Attn: Dr. R. C. Ohlman (1 copy)

ILC Laboratories, Inc., 164 Commercial Street, Sunnyvale, CA 94086, Attn: L. Noble (1 copy)

University of Texas at Dallas, P. O. Box 30365, Dallas, TX 75230, Attn: Professor Carl B. Collins (1 copy)

Director, Defense Advanced Reasearch Projects Agency, 1400 Wilson Boulevard, Arlington, Virginia, Attn: Program Management (2 copies)

Director, Naval Research Laboratory, Washington, D. C. 20375, Attn: Code 2629 (6 copies)
Code 2627 (6 copies)